LLNL-TR-655420

Military Interdepartmental Purchase Request: MIPR1EO89M1115

Integrated Detection of Pathogens and Host Biomarkers for Wounds

Technical Point of Contact Information
Name: Crystal Jaing
Email: jaing2@llnl.gov
Phone: (925) 424-6574
Address: 7000 East Avenue
Mail Code 174
Livermore, CA 94550

This document was prepared as an account of work sponsored by an agency of the United States government. Neither the United States government nor Lawrence Livermore National Security, LLC, nor any of their employees makes any warranty, expressed or implied, or assumes any legal liability or responsibility for the accuracy, completeness, or usefulness of any information, apparatus, product, or process disclosed, or represents that its use would not infringe privately owned rights. Reference herein to any specific commercial product, process, or service by trade name, trademark, manufacturer, or otherwise does not necessarily constitute or imply its endorsement, recommendation, or favoring by the United States government or Lawrence Livermore National Security, LLC. The views and opinions of authors expressed herein do not necessarily state or reflect those of the United States government or Lawrence Livermore National Security, LLC, and shall not be used for advertising or product endorsement purposes.

This work performed under the auspices of the U.S. Department of Energy by Lawrence Livermore National Laboratory under Contract DE-AC52-07NA27344.

AD_____

Military Interdepartmental Purchase Request: MIPR1EO89M1115

TITLE: Integrated Detection of Pathogens and Host Biomarkers for Wounds

PRINCIPAL INVESTIGATOR: Crystal Jaing

CONTRACTING ORGANIZATION: Lawrence Livermore National Laboratory

REPORT DATE: April 24, 2014

TYPE OF REPORT: Final

PREPARED FOR: U.S. Army Medical Research and Materiel Command
Fort Detrick, Maryland 21702-5012

DISTRIBUTION STATEMENT: Distribution authorized to U.S. Government agencies only (proprietary information, (Month and Year). Other requests for this document shall be referred to U.S. Army Medical Research and Materiel Command, 504 Scott Street, Fort Detrick, Maryland 21702-5012

The views, opinions and/or findings contained in this report are those of the author(s) and should not be construed as an official Department of the Army position, policy or decision unless so designated by other documentation.

REPORT DOCUMENTATION PAGE

Form Approved
OMB No. 0704-0188

Public reporting burden for this collection of information is estimated to average 1 hour per response, including the time for reviewing instructions, searching existing data sources, gathering and maintaining the data needed, and completing and reviewing this collection of information. Send comments regarding this burden estimate or any other aspect of this collection of information, including suggestions for reducing this burden to Department of Defense, Washington Headquarters Services, Directorate for Information Operations and Reports (0704-0188), 1215 Jefferson Davis Highway, Suite 1204, Arlington, VA 22202-4302. Respondents should be aware that notwithstanding any other provision of law, no person shall be subject to any penalty for failing to comply with a collection of information if it does not display a currently valid OMB control number. **PLEASE DO NOT RETURN YOUR FORM TO THE ABOVE ADDRESS.**

1. REPORT DATE
04-24-2014

2. REPORT TYPE
Final

3. DATES COVERED
March 22, 2011 – March 31, 2014

4. TITLE AND SUBTITLE

Integrated Detection of Pathogens and Host Biomarkers for Wounds

5a. CONTRACT NUMBER
MIPR1EO89M1115

5b. GRANT NUMBER
DM102734

5c. PROGRAM ELEMENT NUMBER

5d. PROJECT NUMBER

5e. TASK NUMBER

5f. WORK UNIT NUMBER

6. AUTHOR(S)

Crystal Jaing, Nicholas Be, Kevin McLoughlin, Jonathan Allen, Shea Gardner, Brett Chromy, Paul Luciw, Trevor Brown, Eric Elster

7. PERFORMING ORGANIZATION NAME(S) AND ADDRESS(ES)

Lawrence Livermore National Laboratory
7000 East Avenue, Livermore, CA 94550

University of California, Davis
One Shields Avenue Davis, CA 94518

8. PERFORMING ORGANIZATION REPORT NUMBER

9. SPONSORING / MONITORING AGENCY NAME(S) AND ADDRESS(ES)
U.S. Army Medical Research and Materiel Command
Fort Detrick, Maryland 21702-5012

10. SPONSOR/MONITOR'S ACRONYM(S)

11. SPONSOR/MONITOR'S REPORT NUMBER(S)

12. DISTRIBUTION / AVAILABILITY STATEMENT
Distribution authorized to U.S. Government agencies only (proprietary information, (Month and Year).
Other requests for this document shall be referred to U.S. Army Medical Research and Materiel Command, 504 Scott Street, Fort Detrick, Maryland 21702-5012

13. SUPPLEMENTARY NOTES

14. ABSTRACT

The increasing incidence and complications arising from combat wounds has necessitated a reassessment of methods for effective treatment. Infection, excessive inflammation, and incidence of drug-resistant organisms all contribute toward negative outcomes for afflicted individuals. The organisms and host processes involved in wound progression, however, are incompletely understood. We therefore set out, using our unique technical resources, to construct a profile of combat wounds. We employed the Lawrence Livermore Microbial Detection Array and next-generation sequencing to identify all microorganisms present in wound samples, building complete profiles of wound infection. These methods allowed for comprehensive assessment of the wound bioburden, revealing pathogens that could not be detected by standard microbiology. Further, we developed and applied proteomics technology and identified host biomarkers associated with wound resolution. In combination with our pathogen data, these biomarker discovery efforts will provide a profile that will assist in clinical outcome classification and will provide vital insight for treatment of these complex cases.

15. SUBJECT TERMS
Wound infection, biomarker, nosocomial pathogen, host-pathogen interaction

16. SECURITY CLASSIFICATION OF:			**17. LIMITATION OF ABSTRACT**	**18. NUMBER OF PAGES**	**19a. NAME OF RESPONSIBLE PERSON**
					USAMRMC
a. REPORT	**b. ABSTRACT**	**c. THIS PAGE**			**19b. TELEPHONE NUMBER** *(include area code)*
U	U	U	UU	35	

Table of Contents

	Page
Introduction……..…	**4**
Body: Research methods and results……	**4**
Aim 1……	**4**
Aim 2……	**10**
Aim 3……	**21**
Key Research Accomplishments……..	**25**
Reportable Outcomes……	**26**
Conclusion……	**27**
References……	**28**
Supporting Data……	**30**

INTRODUCTION

Modern combat environments present many unique and difficult challenges relevant to medical treatment of injured warfighters. Improvised explosive devices, increasing number and severity of injuries per casualty, longer patient transport times, and higher died-of-wound rates necessitate a reassessment of our approach to wound treatment. Although it has been shown that both infection and subsequent inflammatory pathology play an important role in wound progression, objective criteria for assessing and accurately estimating the likelihood of successful wound healing have yet to be clearly established (1-3).

Previous studies of wound infection have focused on a small subset of well-characterized pathogens (4, 5). Analyses of chronic wounds have shown that the wound microflora is composed of a spatially-structured (6-8) community of organisms that impacts healing through host immune and inflammatory responses (2, 9). Many of these organisms may be difficult or impossible to culture under standard conditions, and their role in colonization of acutely wounded tissue is not well understood. In acute wounds, it is possible that organisms undetected by conventional techniques may impact the inflammatory response and play a significant role in the healing process. This process is highly regulated, involving hemostasis, inflammation, cell proliferation, and tissue remodeling. Failed wounds do not progress through these normal stages, thus biomarkers for these processes could be predictive of the healing response (1-3, 10).

Construction of a comprehensive panel of host response biomarkers, in combination with a microbial profile of corresponding wounds, could provide actionable metrics with high utility for clinical case management of complex combat wounds. Toward this end, we assembled a collaborative and experienced team, combining the extensive clinical wound research expertise and the unique wound sample collection from the Naval Medical Research Center (NMRC), the advanced and proven bioinformatics and pathogen detection expertise from the Lawrence Livermore National Laboratory (LLNL), and the proteomic and biomarker research expertise from the University of California, Davis to conduct a comprehensive characterization of microorganisms and host proteins associated with wound outcome. Comprehensive microbial detection was performed using a combination of novel microarrays and whole genome sequence analysis. Protein biomarker identification was performed using an optimized 2-D difference gel electrophoresis (2D DIGE) system. These unique discovery platforms have produced novel biomarker data for design of diagnostics that could reduce morbidity and improve quality of life for injured service members.

BODY: RESEARCH METHODS AND RESULTS

AIM 1: DETECTION OF MICROBIAL PATHOGENS IN WOUNDS (LLNL, NMRC)

Task 1. LLNL will analyze nucleic acid extracts provided by DOD collaborators from a maximum of 25 wound patient samples per year (for each of three years) from combat wounds by utilizing a microbial discovery array platform for viruses, bacteria, fungi and protozoa in these samples.

Sample collection. Tissue and effluent samples were collected from 124 debridement procedures representing 61 wounds in 44 combat-injured service member patients evacuated to the National Capital Area from Iraq and Afghanistan. Each sample was assigned an identifier with three components: patient ID number, wound number, and sample type (eg. 1-1-WA). Tissue biopsies

were designated as “W” and effluent as “E.” Samples were obtained from up to three procedures per wound (designated A, B, C). The annotation “ON” indicates an effluent sample was collected overnight starting the evening before debridement, while “2” indicates the effluent was collected for two hours following the procedure.

Nucleic acid processing. Wound samples were homogenized and DNA extracted using the QiaAMP DNA Mini Kit and QIAamp cador Pathogen Mini Kit according to the manufacturer’s recommendations. Tissue samples of 15-20 mg were cut into small pieces and digested via incubation in proteinase K. Samples were disrupted via high-speed vortexing with 0.1 mm zirconia beads to facilitate disruption of gram-positive bacteria. Purification of nucleic acid from sample homogenate was performed using QiaAMP spin columns. DNA fluorescent labeling was performed using the Nimblegen One-Color DNA Labeling Kit (Roche, Indianapolis, IN) according to the manufacturer’s instructions. Labeled DNA was purified via isopropanol precipitation and resuspended in water for microarray hybridization.

Microarray hybridization and analysis. This study employed the Lawrence Livermore Microbial Detection Array (LLMDA), which contains probes designed for detection of 1856 viral, 1398 bacterial, 123 archaean, 48 fungal, and 94 protozoan species. DNA samples were prepared for hybridization using the Nimblegen Hybridization Kit LS. Ten µg labeled DNA was hybridized to each array, followed by incubation for 45-60 hours at 42°C. Arrays were washed and scanned at 2 µm resolution. Resultant data were analyzed using an automated composite likelihood maximization method developed at LLNL (11). Probe intensity thresholds were set at either the 99th or 95th percentile above negative control probes, as indicated in the following data.

Microorganisms detected in wound samples by LLMDA. The LLMDA version 5 was applied for analysis of 124 wound samples, obtained from 61 wounds in 44 patients. Of these samples, 63 tested positive for one or more microorganisms (51%) (Supporting data, Table S1). Thirty-nine samples (31% of total) were indicated to contain more than one microbial species. Select samples had also been previously interrogated for bacterial presence via quantitative culture as part of a separate ongoing study at NMRC. Of the 82 culture-negative samples, 28 (34% of culture negative samples) were indicated to contain at least one microbial species. The most commonly observed microbial species in wound samples was *Acinetobacter baumannii*, represented in 28 samples (23% of total) (Figure 1).

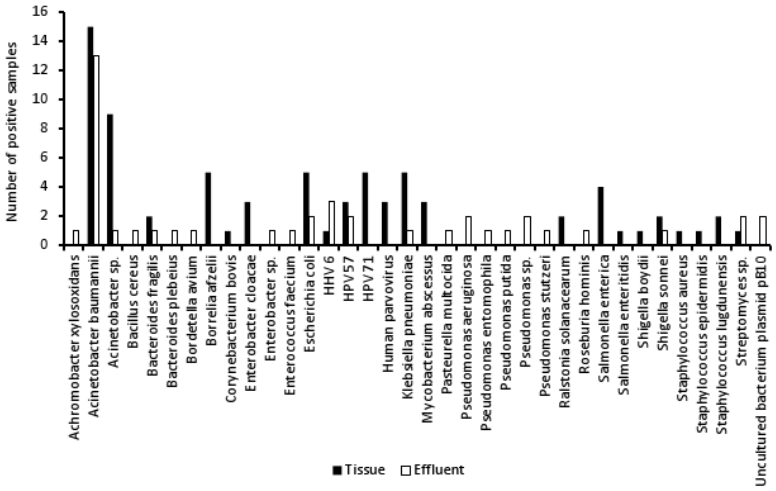

Figure 1. Microorganisms detected in wound tissue or effluent by LLMDA.

Some cases were also observed in which a cultured organism was not detected by microarray analysis. This may have been due to inherently reduced capacity of the array to identify some organisms depending on quality and annotation of the corresponding reference genomes. It is also possible that further optimization of extraction protocols, particularly as applied to difficult-to-lyse gram-positive bacteria, could improve DNA yield and detection capacity. Also, the culture and molecular analyses were performed on different sample aliquots, thus it is possible that microbes may not have been homogenously distributed in the tissue/effluent. Discrepancies between culture-based and molecular techniques have similarly been observed in chronic wound studies, where results derived from distinct detection modalities depended on the bacterial group in question (12). These observations reinforce the difficulty in exclusive use of a single diagnostic tool, and indicate that complementary approaches may be useful for yielding fully comprehensive results.

Task 2. LLNL will work with DOD collaborators to further investigate 5 samples per year by deep metagenomic sequencing of wound samples initially characterized by the discovery array.

Next-generation sequencing and analysis. Sequencing was performed at the California Institute for Quantitative Biosciences, Vincent J. Coates Genomics Sequencing Laboratory. DNA samples were processed on the Illumina Hiseq 2000 platform using 100 bp paired-end reads, multiplexing three samples in each flow cell lane. Whole genome sequencing was performed to capture information from all bacterial, plasmid, viral, and fungal sequence data. Resultant data were processed using the Livermore Metagenomics Analysis Toolkit (LMAT), a platform developed at LLNL for taxonomy classification using a unique reference genome database.

Bacteria detected by next-generation sequencing. DNA extracted from a subset of 21 wound samples was subjected to whole genome sequencing and analyzed using the Livermore Metagenomics Analysis Toolkit (LMAT) (13). Results revealed a broad range in mapped microbial sequence data between individual wound samples. However, when samples were placed in a heatmap and ordered according to their corresponding microbial profiles, samples from wounds with similar outcomes did not group together significantly (Figure 2A). Figure 2B

represents a subset of the most frequently detected microorganisms. Samples derived from the same patient did not associate as closely as when all detected organisms were considered, indicating that inclusion of all detected organisms may be more clinically relevant. In one particular case in which multiple sampling timepoints were available (patient 26), samples obtained from the same wound at different times were observed to be compositionally distinct (Figure 2C).

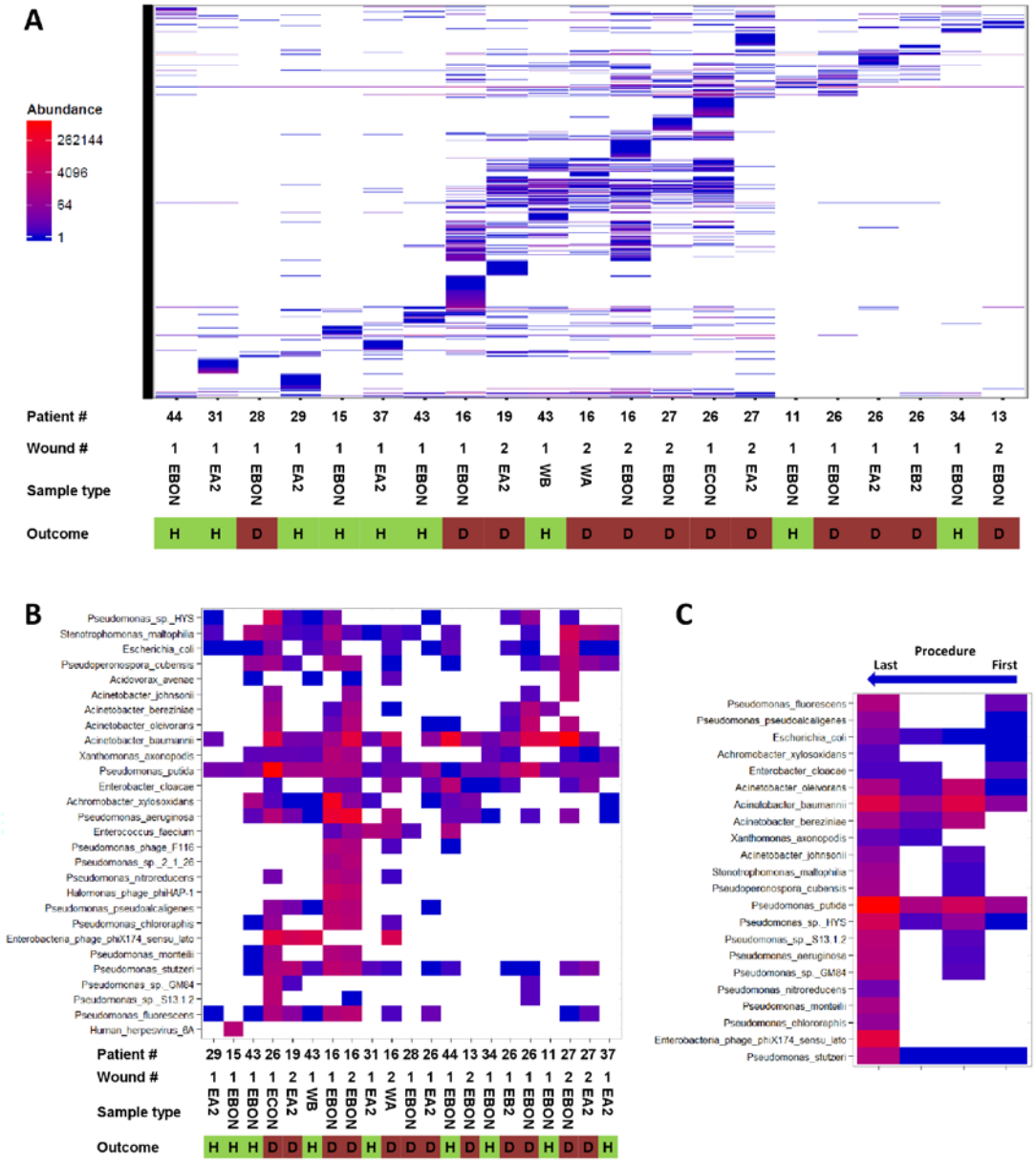

Figure 2. Distribution of microorganisms detected in wound samples by analysis of next-generation sequence data. Individual wound samples given in columns with wound outcome (H = healed, D = dehisced). Microbial species shown along vertical axis. **A.** Heatmap showing all microbial species detected. **B.** Heatmap showing only top microbial species (1000 or more total reads assigned). **C.** Heatmap showing top microbial species for patient 26.

Fungi and viruses detected in wounds by next-generation sequencing. One of the advantages of a whole genome approach is the ability to detect fungal and viral sequences in addition to bacteria. Fungal species identified in wound samples above the set threshold included *Aspergillus terreus, Aspergillus nidulans, Alternaria arborescens, Saccharomyces cerevisiae, Malassezia restricta, Pseudoperonospora cubensis,* and *Neosartorya fischeri* (Table 1, see publication Be et al. for complete analysis parameters and cutoffs). *Aspergillus* were detected in all samples derived from patient 26, whose wounds failed to heal. *Aspergillus* were also observed in one other sample derived from a failed wound and one from a healed wound. Although less common than bacterial colonization *Aspergillus* infections have been associated with combat injury, complicating wound care, and early detection could improve care in these cases.

Due to low coverage, viral presence could only be reliably verified in three samples (Table 1). Notably, *Pseudomonas* phage was observed in samples obtained from both wounds in patient 16, corresponding to *Pseudomonas* detection via LLMDA. Further assessment of wound bacteriophage communities could be relevant to future development of novel phage therapy for addressing drug-resistant *A. baumannii* and *P. aeruginosa* infections (14, 15).

Sample	Wound outcome	Total reads	Strain-specific reads	Mean match score	Species/strain
			Fungi		
29-1-EA2	Healed	1307	38	2.12	Malassezia restricta CBS 7877
43-1-EBON	Healed	27	25	2.65	Aspergillus terreus NIH2624
		76	60	2.31	Aspergillus nidulans FGSC A4
		27	19	2.28	Alternaria arborescens EGS 39-128
		1193	74	1.65	Pseudoperonospora cubensis
43-1-WB	Healed	208	26	2.51	Saccharomyces cerevisiae
26-1-EA2	Dehisced	145	134	2.26	Aspergillus terreus NIH2624
26-1-EBON	Dehisced	35	29	2.26	Aspergillus terreus NIH2624
26-1-EB2	Dehisced	70	68	2.40	Aspergillus terreus NIH2624
26-1-ECON	Dehisced	39	34	2.33	Aspergillus terreus NIH2624
27-2-EA2	Dehisced	2281	37	2.75	Aspergillus terreus NIH2624
		118	47	1.91	Pseudoperonospora cubensis
27-2-EBON	Dehisced	3458	1653	1.70	Pseudoperonospora cubensis
		35693	36	1.68	Neosartorya fischeri NRRL 181
			Viruses		
15-1-EBON	Healed	1346	1212	2.52	Human herpesvirus 6A
16-1-EBON	Dehisced	2219	843	1.72	Pseudomonas phage F116
		7972	348	1.57	Pseudomonas phage phiCTX
16-2-EBON	Dehisced	3042	461	1.78	Pseudomonas phage phiCTX

Table 1. Fungi and viruses identified in wound samples through sequence analysis.

Strain genotyping based on next-generation sequence analysis. The relatively high sequence coverage for *Acinetobacter baumannii* in some samples raised the possibility of identifying the strain associated with infection. Sequence alignment and unique SNP-based identification approaches (16, 17) were therefore applied for strain resolution. Attempts were made to identify the infecting *A. baumannii* strain in each sample with sufficient sequence data using both SNP and read-based sequence analysis. Notably, six of the dehisced samples grouped together and were distinct from all other strains, clustering more tightly within these samples

than to any single assembled genome (Table 2). Based on LMAT mapping, strain Naval-18 demonstrated the closest association to this cluster. It was not possible, for the available samples in which SNPs were detected, to identify distinct SNPs shared by healed samples that differed from all dehisced samples. Enhancement of coverage could, however, facilitate identification of strains with non-random associations between healed and failed wounds.

		kSNP analysis		LMAT sequence mapping analysis		
Sample	**Outcome**	**# SNPs (k=19)**	**Closest strain**	**Number of strain-specific reads**	**Closest strain**	**Fraction of genome covered by total reads**
11-1-EBON	Healed	282922	ANC_4097	18,210	AB058	1
34-1-EBON	Healed	0	N/A	4	AB058	0.0008
44-1-EBON	Healed	285432	IS-123	6	TG2026	1
13-2-EBON	Dehisced	101	AB4857	N/A	None	0.0019
16-1-EBON	Dehisced	1041	Wound cluster	13	Naval-18	0.0274
16-2-EBON	Dehisced	268716	Wound cluster	4,267	Naval-18	0.6178
16-2-WA	Dehisced	302	6013113	7	6013150	0.0737
26-1-EA2	Dehisced	468	Wound cluster	7	Naval-18	0.0089
26-1-EB2	Dehisced	1245	Wound cluster	19	Naval-18	0.0516
26-1-EBON	Dehisced	274540	Wound cluster	6,057	Naval-18	1
26-1-ECON	Dehisced	231404	Wound cluster	2,668	Naval-18	0.5489
27-2-EA2	Dehisced	43	Ab33333	N/A	None	0.0009
27-2-EBON	Dehisced	295037	6013150	26,429	6013150	1

Table 2. *Acinetobacter baumannii* strains with closest genetic distance to wound samples.

Task 3. LLNL will develop multiplex PCR signatures for bacterial strains determined by consultation with DOD collaborators. PCR primers and probes will be developed for *Acinetobacter* with detection of *A. baumannii*, *P. aeruginosa*, *S. aureus* with detection of MRSA, *Streptococcus* (β-hemolytic group C), and *K. pneumonia*.

Computational design of PCR assays for microbial detection. A subset of microbial organisms detected in this study was selected for signature analysis. PCR signatures were designed for the viruses detected using the run_Primux_triplet script that is part of the PriMux software (18) developed at LLNL. Predicted targets were identified using simulate_PCR (submitted, https://sourceforge.net/projects/simulatepcr) based on comparison to the LLNL large internal database of all available finished and assembled microbial genomes from NCBI, multiple public and university sequencing centers and from collaborators, currently over 75 GB of sequence data, as well as the NCBI nt database. PCR signatures were computationally developed for *Acinetobacter baumannii*, *Acinetobacter* plasmid pRAY, *Pseudomonas*, gastroenteric bacteria that demonstrated significant associations with wound outcome (*Bacteroides*, *Enterobacter*, *Escherichia coli*, *Enterococcus*, *Salmonella*), *Klebsiella pneumonia*, and *Shigella sonnei*. These signatures could be used for rapid detection of these organisms in clinical samples. Signatures are available upon request.

The above results, all of which are outlined in a manuscript currently under review (Be et al. 2014) underscore the importance of supplementing existing microbiological techniques with more comprehensive molecular protocols for microbial detection. The ability to comprehensively identify

bacteria, fungi, and viruses associated with a wound would be a tremendous advantage in management of individual cases. Further, the corresponding genotype data could provide relevant information on virulence and antimicrobial resistance. These platforms would facilitate treatment of infections not identifiable by standard culture, providing clinicians with invaluable information during the debridement process.

Technical challenges and practiced mitigation

1. Sample preparation methods initially applied early in this project were deemed non-ideal for nucleic acid analysis due to incomplete homogenization of the sample and protocols that may not have been sufficient for complete disruption of gram-positive bacteria. More extensive disruption protocols were therefore applied, including thorough bead beating, high-speed vortexing, and high temperature proteolytic lysis.
2. When subjected to sequencing, DNA extracts derived from wound tissue samples yielded high percentages (>99%) of human DNA sequence data. Subsequent sequencing runs prioritized effluent samples, expected to demonstrate larger percentages of bacterial sequence data, in addition to being more accessible in a clinical environment.

AIM 2: IDENTIFICATION OF BIOMARKERS FOR HOST REPONSES IN COMBAT WOUNDS (UC DAVIS, NMRC)

Task 4. A proteomics approach, based on 2-dimensional differential gel electrophoresis (2-D DIGE), will be applied for the discovery of novel biomarkers in wound exudates, debridement tissue, and plasma of patients.

Optimization of 2-D difference gel electrophoresis. Biomarker discovery from combat wounds was assessed using 2-D difference gel electrophoresis (2-D DIGE). Using 2-D DIGE, we were able to identify proteins observed at significantly different levels between healed and non-healing wounds. In order to optimize our methods, we performed studies using samples which were likely to be similar to those obtained from combat wounds. We conducted proteomics experiments by determining the optimal sample preparation method for proteomic analysis of burn wounds. Freshly obtained normal and burn skin was subjected to a single freeze/thaw cycle. Although differences were seen between frozen and fresh tissue, discrepancies were minor and, due to the likely difficulty in obtaining fresh tissue for this project, differences were deemed acceptable. Moreover, we compared three other lysis methods, namely, bead beating, chemical tissue disruption (T-PER), and mechanical disruption. All four methods were successful and showed that site to site variation in overall protein content and specifically in the amount of albumin is substantial. We submitted this manuscript for review, but it was rejected. We are currently repeating some experiments and expect to resubmit this manuscript soon. Additional proteomic optimization was completed for both serum and wound effluent from samples received from combat-injured service member patients evacuated to the National Capital Area from Iraq and Afghanistan. Knowledge gained from the skin sample preparation work, helped guide our experiments for these more numerous and complex samples.

Protein level observations. In our preliminary proteomic sample preparation studies, we detected a large number of protein spots and a fair number of differentially expressed spots when

comparing healthy and burn wound tissue. We detected over 600 protein spots, and several were found to be differentially expressed between healthy and burn tissue, as well as different between burn tissue with and without collection of a fatty layer of tissue. Although differences between the four methods used, we analyzed the amount of tissue needed from each sample for this study, and found that 500 ug of tissue will be sufficient regardless of the sample preparation chosen.

Most importantly, we established an appropriate sample preparation method for obtaining high quality protein spot maps for healthy and burn wound human skin tissue. Several techniques were evaluated and compared including glass bead homogenization and chemical lysis using freeze/thaw cycles. Glass bead homogenization is likely the most appropriate for the sample size and sample status of any granulated tissue from NMRC that we may obtain. In addition, we examined the proteomic differences between different skin regions on the same individual and healthy tissue between two individuals. Skin regions from the same individual varied according to location on the same individual, so we had to obtain similar skin pieces in order to directly compare the different techniques. However, as expected, the differences between two individuals showed the most dramatic differences in proteomic content. These results strengthen the need to examine multiple samples from the same individual (samples collected over time) to truly understand the patient-to-patient variability in wound samples.

In addition to the skin samples obtained at UC Davis, we received 75 effluent and 49 serum samples in two different shipments from NMRC. Each sample contains 2 mLs of material. We have assessed protein concentration in 48 effluent samples and all 49 serum samples. These same samples were analyzed all by SDS-PAGE; effluent looks very similar to serum. Protein concentration ranges: Effluent: 14 – 88 mg/ml; Serum: 33 – 63 mg/ml. We determined that it was necessary to remove high abundant protein from effluent, similar to our previous affinity chromatography methods for removal in serum Figure 3. We removed high abundant proteins from these 48 effluent samples and all 49 serum samples. High abundant protein removal from both sample types benefits overall proteome appearance and aids in biomarker discovery. This work was part of the basis for one of our published manuscripts during this project (19). The paper, entitled “Proteomic Sample Preparation for Blast Wound Characterization”, is a method development paper for high abundant protein depletion for both wound effluent and serum samples. This is the first study to show a successful method for high abundant protein depletion from wound effluent which is compatible with downstream 2-D DIGE analysis. This development allows for improved biomarker discovery in wound effluent and serum samples.

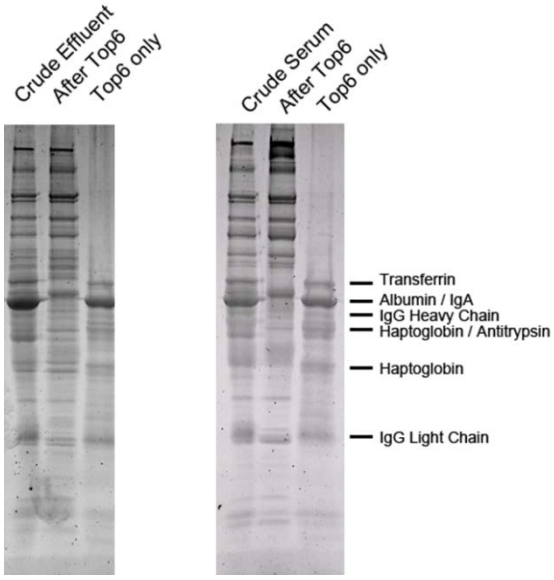

Figure 3. **SDS-PAGE showing effective removal of high abundant proteins and an improved protein pattern suitable for 2-D DIGE applications**. (Left) An effluent sample was run before and after high abundant protein removal. Crude effluent shows several very intense protein bands, reducing the total number of proteins detected. The lower abundant fraction (middle lane) shows an appropriate protein pattern for 2-D DIGE biomarker discovery. The right lane shows the high abundant proteins eluted off the affinity chromatography column that were separated from

the lower abundant fraction. The identical results were obtained for the serum samples (right panel).

Using this approach for biomarker discovery, a subsequent biomarker analysis and biomarker panel was published in 2013 (20) using 44 of the wound effluent samples. This approach identified 52 protein spots that were differentially expressed and thus represent candidate biomarkers for this clinical application. Many of these proteins are intimately involved in inflammatory and immune responses. Furthermore, discriminate analysis further refined the 52 differential protein spots to a smaller subset of which successfully differentiate between wounds that will heal and those that will fail and require further surgical intervention with greater than 83% accuracy. These results suggest candidates for a panel of protein biomarkers that may aid traumatic wound care prognosis and treatment.

To improve successful mass spectrometry identification of putative host protein biomarkers, we ran a ‘pick’ gel that contains additional protein as compared to the amount normally contained in 2D gels (Figure 4). Comparison results of healed vs. dehisced, culture status (positive vs. negative) and the presence of bacteria as determined the LLMDA were individually characterized and collectively reveals 122 protein spots with greater than 1.2 fold change and p-value < 0.05. Of the 122 proteins among the 3 comparisons, 52 proteins were found for this comparison and 45 proteins were successfully identified (20). These proteins are shown in Table 3. For culture status, 74 proteins were found and 62 protein spots were successfully identified (Table 4).

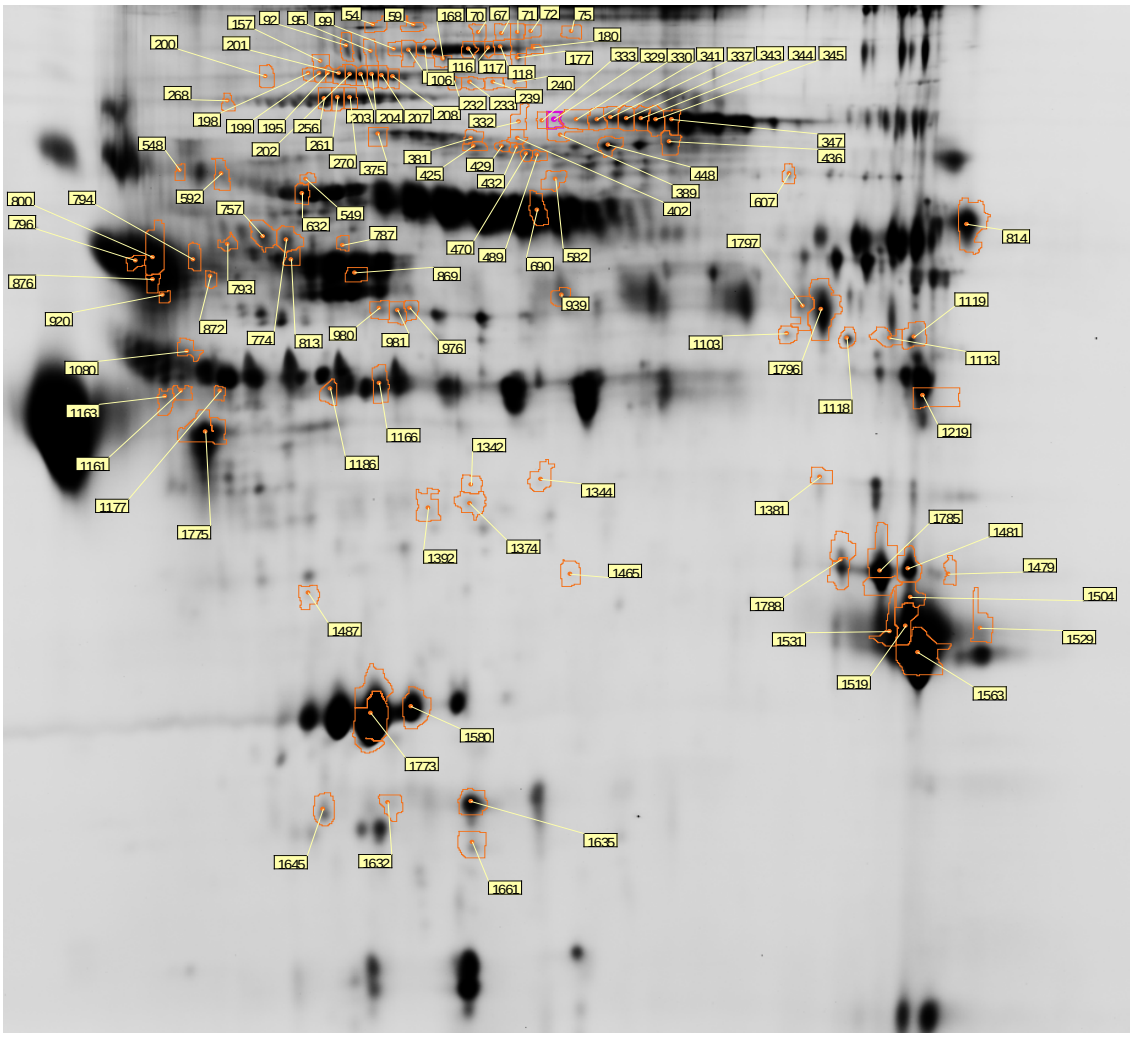

Figure 4. Gel image of 'pick' gel used to determine differentially expressed protein spots from comparisons between healed and dehisced wounds, culture positive and culture negative and bacterial positive and bacterial negative. Each spot boundary is defined in orange and labeled with assigned spot number. There are 122 protein spots here representing protein spots that differ by at least 1.2 fold and have p values of less than 0.05.

Spot No.	IPI No.	Protein Name	Mascot Score	Fold Change (Healed/ Dehisced)	T-test	Th. MW	Th. pI
59	IPI00440484	PER1 - Period Circadian protein homolog 1	133	-1.23	0.04140	137667	5.73
95*	IPI00645206	PCDH17 - Isoform 1 of Protocadherin 17	131	-1.22	0.01210	127405	5.03
99*	IPI00235407	STK36 - Isoform 1 of Serine/threonine protein kinase 3	142	-1.24	0.00176	145728	5.57
102	IPI00185661	USP32 – Ubiquitin carboxyl terminal hydrolase 32	125	-1.2	0.01640	145671	6.18
106	IPI00470744	PARG - Isoform 2 of Poly (ADP-ribose) glycohydrolase	113	-1.22	0.01060	103503	5.58
168*	IPI00290328	PTPRJ- Receptor type tyrosine protein phosphotase precursor	130	-1.51	0.00610	152960	5.80
195*	IPI00017601	CP - Ceruloplasmin	101	-1.27	0.01160	122983	5.44
198*	IPI00017601	CP - Ceruloplasmin	121	-1.39	0.00763	122983	5.44
199	IPI00017601	CP - Ceruloplasmin	182	-1.31	0.00946	122983	5.44
200	IPI00017601	CP - Ceruloplasmin	116	-1.33	0.00751	122983	5.44
201	IPI00017601	CP - Ceruloplasmin	112	-1.3	0.02540	122983	5.44
202	IPI00017601	CP - Ceruloplasmin	154	-1.31	0.01300	122983	5.44
329	IPI00011736	PIK3R2 - Phosphatidylinositol 3 kinase regulatory subunit 2	88	1.26	0.02590	81837	6.03
330	IPI00783987	C3 - Complement C3	115	1.55	0.00034	188569	6.02
333	IPI00011736	PIK3R2 - Phosphatidylinositol 3 kinase regulatory subunit 2	111	1.25	0.00464	81837	6.03
337	IPI00783987	C3 - Complement C3	88	1.53	0.01040	188569	6.02
341*	IPI00783987	C3 - Complement C3	147	1.56	0.00064	188569	6.02
343*	IPI00783987	C3 - Complement C3	189	1.62	0.00063	188569	6.02
344	IPI00783987	C3 - Complement C3	120	1.69	0.00481	188569	6.02
345	IPI00783987	C3 - Complement C3	79	1.59	0.01250	188569	6.02
347	IPI00783987	C3 - Complement C3	104	1.52	0.03390	188569	6.02
375*	IPI00607814	XPNPEP1 - Xaa-Pro aminopeptidase 1 Isoform 2	121	1.23	0.04150	72746	5.67
389	IPI00157535	EPS8L1 - Isoform 4 of Epigrowth factor receptor kinase subunit 8	118	1.23	0.01680	88920	6.49
436	IPI00009089	FRS3 - Fibroblast growth factor receptor substrate 3	121	-1.28	0.01980	55169	6.81
582	IPI00301255	IGSF21 - Immunoglobulin superfamily member 21	109	-1.23	0.04800	51855	6.48
602	IPI00329555	F7 - Isoform A of Coagulation factor VII	178	-1.54	0.02320	53043	6.91
607	IPI00329555	F7 - Isoform A of Coagulation factor VII	130	-1.37	0.04620	53043	6.91
787	IPI00021891	FGG – Fibrogen gamma chain 1	135	1.33	0.02670	51511	5.37
794	IPI00847635	SERPINA3 - Isoform 1 of alpha-1-antichymotrypsin	146	1.57	0.00671	47792	5.33
800	IPI00847635	SERPINA3 - Isoform 1 of alpha-1-antichymotrypsin	216	1.22	0.02730	47792	5.33
814	IPI00219330	ILF3 - Isoform 5 of Interleukin enhancer binding factor 3	252	-1.35	0.02050	74959	8.40
869	IPI00783625	SERPINB5 - Isoform 1 of Serpin B5	120	1.27	0.03560	42530	5.72
872*	IPI00847635	SERPINA3 - Isoform 1 of alpha-1-antichymotrypsin	111	1.39	0.04560	47792	5.33
876	IPI00847635	SERPINA3 I- soform 1 of alpha-1-antichymotrypsin	283	1.24	0.04240	47792	5.33
976	IPI00004657	HLA-B - HLA class 1 histocompatibility antigen	102	1.27	0.01500	40777	5.57
980	IPI00004657	HLA-B - HLA class 1 histocompatibility antigen	121	1.34	0.03830	40777	5.57
981	IPI00004657	HLA-B - HLA class 1 histocompatibility antigen	101	1.57	0.00077	40777	5.57
1080	IPI00166729	AZGP1 - Zinc alpha 2 glycoprotein precursor	147	-1.34	0.00310	34258	5.71
1177	IPI00555812	GC - Vitamin D binding protein precursor	104	-1.28	0.01510	52963	5.40
1186	IPI00641737	HP - Haptoglobin	92	-1.29	0.03740	45205	6.13
1374	IPI00978715	CLU - Clusterin	109	-1.25	0.01060	52494	5.88
1381	IPI00410313	KIR3KL3 - Killer cell immunoglobulin like receptor 3DL3	132	1.25	0.01440	45470	7.27
1392	IPI00022391	APCS - Serum Amyloid P component	181	1.48	0.02230	25837	6.10
1487	IPI00386246	AMPH - Amphiphysin I variant CT3, fragment	119	1.24	0.02510	31195	4.23
1796	IPI00007879	SRF - Serum response factor	132	1.21	0.04600	51592	7.83

Table 3. **Healed vs. Dehisced protein identifications**. The 45 identified differential spots found among biological replicates of healed versus dehisced wounds (corresponding to t-test < 0.05 and fold change cutoff > 1.2) were identified via LC-MS/MS and yielded 25 unique protein identifications. The table includes assigned spot number, IPI database number, protein name, MASCOT identification score, fold change and t-test of expression between healed and dehisced wounds, theoretical molecular weight and pI.
*Indicates the 9 proteins identified as markers by discriminate analysis.

Spot No.	IPI No.	Protein Name	Mascot Score	Fold Change (Healed/ Dehisced)	T-test	Th. MW	Th. pI
54*	IPI00010400	PLCB3 - 1-phosphatidylinositol 4,5-bisphosphate phosphodiesterase beta-3	154	-1.37	0.00318	139511	5.68
59	IPI00440484	PER1 - Period circadian protein homolog 1	133	-1.28	0.02100	137667	5373
67*	IPI00292836	C9 ofr 174 - LOC57653 Isoform 1 of uncharacterized protein	131	-1.53	0.00026	192404	5.74
70	IPI00292836	C9 ofr 174 - LOC57653 Isoform 1 of uncharacterized protein	149	-1.38	0.00072	192404	5.74
71	IPI00292836	C9 ofr 174 - LOC57653 Isoform 1 of uncharacterized protein	133	-1.6	0.00029	192404	5.74
72	IPI00292836	C9 ofr 174 - LOC57653 Isoform 1 of uncharacterized protein	138	-1.29	0.03610	192404	5.74
75	IPI00292836	C9 ofr 174 - LOC57653 Isoform 1 of uncharacterized protein	130	-1.42	0.01860	192404	5.74
92	IPI00291200	NUP133 - Nuclear pore complex protein	141	-1.42	0.01970	129924	4.94
116*	IPI00029739	CFH - Complement factor H	110	-1.23	0.00323	143680	6.21
117	IPI00029739	CFH - Complement factor H	163	-1.24	0.00479	143680	6.21
118*	IPI00029739	CFH - Complement factor H	120	-1.28	0.00439	143680	6.21
157	IPI00025753	DSG1 - Desmoglein-1	128	-1.21	0.01630	114702	4.9
177	IPI00255653	ATP11A - Probably phospholipid transporting ATPase	215	-1.43	0.00407	131155	6.17
180	IPI00029739	CFH - Complement factor H	123	-1.52	0.00495	143680	6.21
199	IPI00017601	CP - Ceruloplasmin	182	-1.34	0.02160	122983	5.44
202*	IPI00017601	CP - Ceruloplasmin	154	-1.3	0.01560	122983	5.44
203	IPI00017601	CP - Ceruloplasmin	203	-1.38	0.01390	122983	5.44
204	IPI00017601	CP - Ceruloplasmin	145	-1.5	0.00541	122983	5.44
207	IPI00017601	CP - Ceruloplasmin	78	-1.4	0.00776	122983	5.44
208	IPI00017601	CP - Ceruloplasmin	111	-1.4	0.00784	122983	5.44
232	IPI00154858	PEAR1 - Platelet endothelial aggregational receptor 1	121	-1.49	0.02120	117661	6.4
233	IPI00154858	PEAR1 - Platelet endothelial aggregational receptor 1	154	-1.56	0.00896	117661	6.4
239	IPI00154858	PEAR1 - Platelet endothelial aggregational receptor 1	104	-1.61	0.01060	117661	6.4
240	IPI00154858	PEAR1 - Platelet endothelial aggregational receptor 1	108	-1.53	0.01440	117661	6.4
256	IPI00896419	ITIH4 - Isoform 1 of Inter-alpha-trypsin inhibitor	90	-1.22	0.00078	103521	6.5
261*	IPI00896419	ITIH4 - Isoform 1 of Inter-alpha-trypsin inhibitor	89	-1.27	0.00011	103521	6.5
270*	IPI00896413	ITIH4 - Isoform 1 of Inter-alpha-trypsin inhibitor	70	-1.32	0.00079	10023	6.06
381	IPI00376782	LILRB3 - Leukocyte immunoglobin-like receptor subfamily B	93	-1.21	0.03440	69385	6.45
425	IPI00219841	LIG1 - DNA Ligase 1	120	-1.44	0.01450	102301	5.49
429	IPI00002564	XRCC1 - DNA repair protein	125	-1.57	0.01810	69776	6.02
549	IPI00020967	LILRB3 - Leukocyte immunoglobin-like receptor subfamily B	102	1.29	0.01780	70819	5.69
632	IPI00020967	LILRB3 - Leukocyte immunoglobin-like receptor subfamily B	91	-1.24	0.04870	70819	5.69
690	IPI00022488	HPX - Hemopexin	176	-1.24	0.01330	52385	6.55
757	IPI00216651	IL28RA - Interleukin 28 receptor subunit alpha	122	1.32	0.03660	58130	4.89
774	IPI00021891	FGG - Fibrinogen gamma chain 1	135	1.32	0.02760	51511	5.37
793*	IPI00019568	F2 - Prothrombinin precursor	177	1.29	0.00667	70036	5.63
796	IPI00847635	SERPINA3 - Isofform 1 of alpha-1-antichymotrypsin	203	1.51	0.03790	47792	5.33
813	IPI00021891	FGG - Fibrinogen gamma chain 1	168	1.34	0.01470	51511	5.37
920	IPI00847635	SERPINA3 - Isofform 1 of alpha-1-antichymotrypsin	81	-1.2	0.04790	47792	5.33
939	IPI00644416	ROR1 - Tyrosine protein kinase transmembrane receptor	118	1.23	0.02840	44825	6.33
1103	IPI00064994	SGCZ - Isoform 2 of Zeta-sacroglycan	118	1.49	0.00563	34872	6.54
1119	IPI00012574	SLC17A2 - Isoform 2 of Na-dependent phosphate transporter protein 3	120	2.72	0.00096	47947	8.73
1161	IPI00166729	AZGP1 - Zinc alpha 2 glycoprotein precursor	100	1.59	0.04270	34258	5.71
1163	IPI00166729	AZGP1 - Zinc alpha 2 glycoprotein precursor	105	1.74	0.04930	34258	5.71
1166	IPI00641737	HP - Haptoglobin	122	-1.56	0.00852	45205	6.13
1342	IPI00978715	CLU - Clusterin	86	1.63	0.00005	37196	5.82
1479	IPI00294405	CLCF1 - Cardiotrophin like cytokine factor 1	128	6.28	0.00073	25388	8.68
1481	IPI00009731	IL25 - Isoform 1 of Interleukin 25	113	4.38	0.00083	20887	8.73
1504	IPI00796435	CA1 - Uncharacterized protein	178	4.39	0.00214	21593	7.1
1519	IPI00796435	CA1 - Uncharacterized protein	218	6.24	0.00220	21593	7.1
1529	IPI00796435	CA1 - Uncharacterized protein	183	6.01	0.00124	21593	7.1
1531	IPI00796435	CA1 - Uncharacterized protein	183	5.44	0.01390	21593	7.1
1563	IPI00796435	CA1 - Uncharacterized protein	282	3.78	0.02750	21593	7.1
1580	IPI00013876	APOBE - Probable DNA dC->dU-editing enzyme	131	-1.28	0.03770	23339	6.34
1632*	IPI0235330	IRGM - Immunity related GTPase family M protein	111	1.48	0.01380	20243	5.23
1635	IPI00553085	LECT1 - Leukocyte cell derived chemotaxin 1	119	3.82	0.00611	14189	5.5
1645*	IPI00300341	TCEB1 - Transcription elongation factor B polypeptide	136	1.52	0.02490	12636	4.74
1661	IPI00956572	TRBC2 - T cell receptor beta-2 chain C region	120	5.54	0.00022	39397	5.26
1773	IPI00853525	APOA1 - Apolipoprotein A1	149	-1.21	0.01580	28005	5.8
1775	IPI00014958	PON2 - Isoform 1 of serum paraoxonase/arylesterase 2	120	-1.2	0.03620	39397	5.26
1785	IPI00718857	IL19RAP - cDNA, similar to Interleukin 18 receptor	128	3.21	0.02810	17558	7.63
1788	IPI00024741	EREG - Proepiregulin	128	3.63	0.01750	19659	7.49

Table 4. **Culture vs. Dehisced protein identifications**. The 62 identified differential spots found among biological replicates of culture negative compared to culture positive (corresponding to t-test < 0.05 and fold change cutoff > 1.2) were identified via LC-MS/MS and yielded 38 unique protein identifications. The table includes assigned spot number, IPI database number, protein name, MASCOT identification score, fold change and t-test of expression between healed and dehisced wounds, theoretical molecular weight and pI. *Indicates the 10 proteins identified as markers by discriminate analysis.

Multivariate statistical analysis (principle component analysis, hierarchical clustering) of the differentially expressed proteins that were able to discriminate between healed and failed wounds was completed and published in Chromy et al, 2013 (20). Principle component analysis and hierarchical clustering were also completed to compare culture status and bacterial detection using quantitative culturing and LLMDA (Figure 5). The clustering of the culture positive samples (black) with culture negative samples (pink) using quantitative culturing cannot be effectively grouped with PCA. However, the LLMDA detection improves the PCA analysis where bacterial positive samples (blue) can more easily be discriminated from bacterial negative samples (yellow). This analysis suggests that the LLMDA may provide a better indication of active pathogen effects and the role of these pathogens in preventing appropriate wound healing.

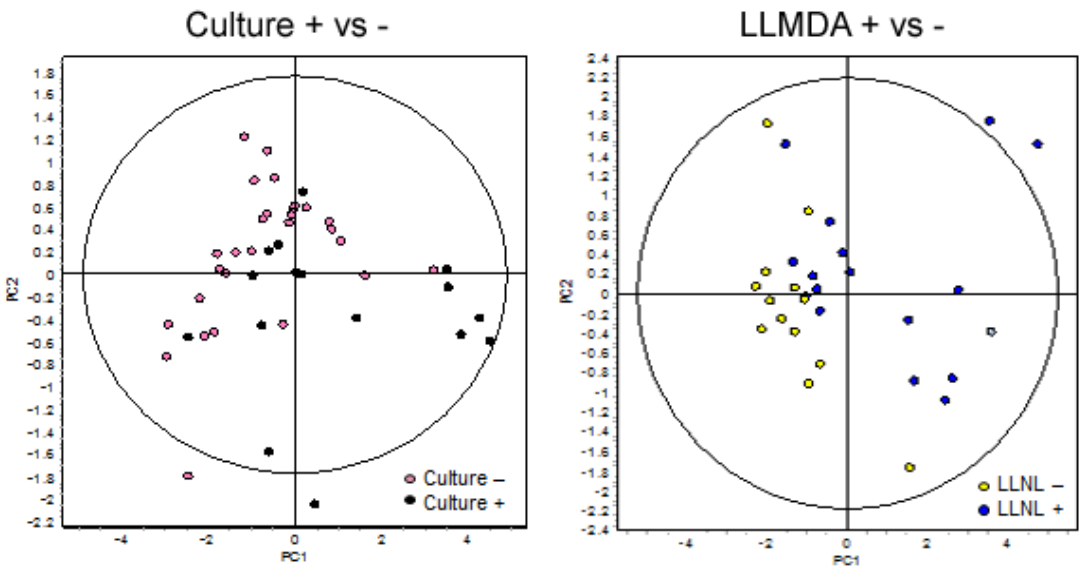

Figure 5. **Principle component analysis shows differences in clustering of host proteome spot maps** comparing culture positive vs. culture negative (left) and LLMDA positive and LLMDA negative samples (right). Protein spot map clustering of bacterial containing samples is improved using LLMDA as compared to culture.

To better understand the differences in the proteins that make these differences between culture positive and culture negative samples, the differential proteins were clustered. The results of the clustering show groups of protein spots that may work in concert to affect proper wound healing (Figure 6).

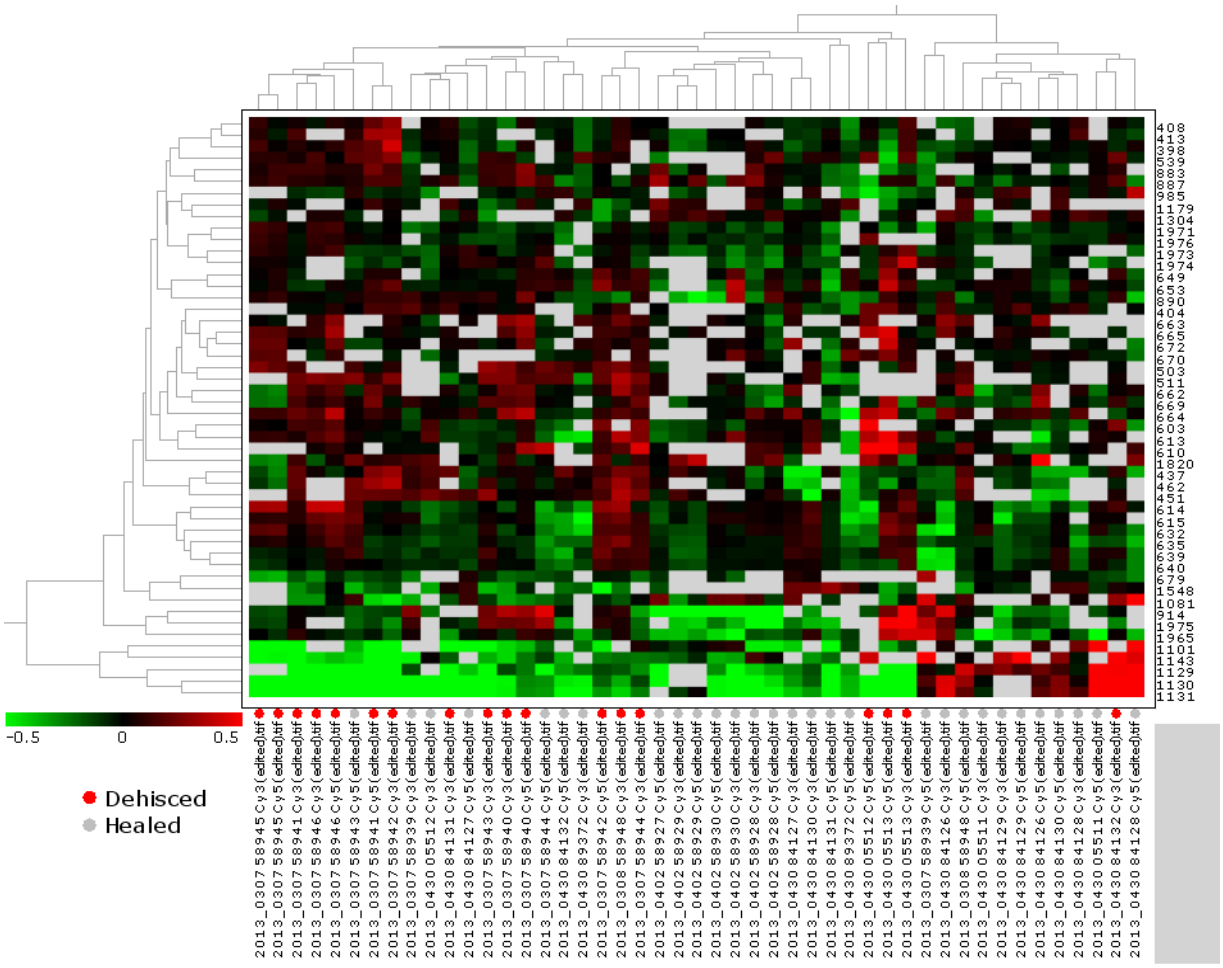

Figure 6. Hierarchical clustering of the 49 serum sample 2-D DIGE experiment is presented as a heat map of protein expression levels. Each protein spot (row) and the clustering of each serum sample used in the experiment (column).

Group	Comparison (left vs. right)		Differential Proteins	Markers selected	Accuracy (%)
1	Healed	Dehisced	52	9	83.83 ± 2.8
2	Culture Negative	Culture Positive	74	10	70.31 ± 16.3
3	LLNL Negative	LLNL Positive	95	6	76.67 ± 7.0

Table 5. **Three groups of comparisons were made using the host proteome dataset**. The total number of differential proteins that were found in each comparison as well as the putative biomarkers that are able to discriminate between the two sample types in each comparison are listed. The percent accuracy of these putative biomarkers are shown. All three are reasonably high, notably the accuracy for the markers using the LLMDA are higher than the accuracy for using culture status as a differentiator.

In addition to the differential proteins that yielded a biomarker panel for discriminating healed and failed wounds in wound effluent, we found 50 differentially expressed protein spots in serum samples. The 50 differential protein spots were used to determine a marker selection panel using the discriminate analysis module of DeCyder EDA. A subset of 13 protein spots was calculated to effectively discriminate between healed and dehisced serum samples, with an accuracy of 84 ± 5.4% (Table 6). These marker selection protein spots provide the best accuracy for differentiating samples. Theoretically, these proteins could be used in a serum 'biomarker' panel to determine which type of sample a particular proteome belongs. In addition, these markers could be used to determine the sample type for an unknown, blind sample.

Group	Serum Comparison (left vs. right)		Differential Proteins	Markers Selected	Accuracy (%)
1	Healed	Dehisced	50	13	84 ± 5.4%

Table 6. Comparison of protein markers in healed and dehisced samples. A total of 13 protein spot markers were selected as discriminators between healed and dehisced sample groups. The percent accuracy of these putative biomarkers are shown and are reasonably high.

We have begun preparing an additional manuscript highlighting the differentially expressed serum proteins that could be used in a biomarker panel for wound healing (see figures above). This paper is very similar in scope and structure as the J. Trans Med. Publication (20), but will be focused on the proteins that change in serum between healed and dehisced wounds.

We assessed the potential for a 'top 14' serum column to remove additional proteins from wound effluent samples to determine if we can preferentially increase the potential protein biomarkers and to determine if we can examine even lower abundant proteins from wound effluent.

Successful removal of the 14 most abundant serum proteins was successful on a pilot experiment using wound effluent. We can now determine if we should use the top 14 column or the top 6 column for future protein biomarker discovery. Initial comparisons of top 14 vs. top 6 removed wound effluent samples showed increased protein spots available following top 14 protein removal. Mass spectrometry identification of proteins that are potential biomarkers between healed and dehisced samples are underway. This pilot work will need to be continued with a larger, statistically valid sample set.

We next compared effluent following removal of the top 14 proteins and compared the data to the samples following top 6 removed wound effluent. More spots were found in the Top14 sample, suggesting additional putative biomarkers might become available using this more comprehensive removal technique. There were 27 protein spots that showed statistically significant differences in protein expression between these samples. Of these, 8 were much higher in the top 6 sample, suggesting these 8 spots were proteins that are contained in the top 14 affinity column and are absent in the top 6 column. Importantly, none of these 8 spots matched up with the putative biomarkers from our top 6 analysis, suggesting that the top 14 column does not 'remove' any putative biomarkers from our previous analysis.

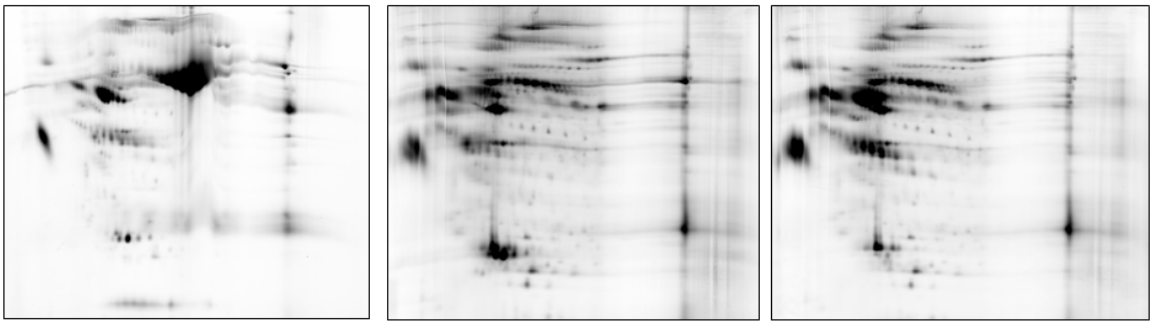

Crude Effluent
1058 Spots

Top 6 Depleted Effluent
1373 Spots

Top 14 Depleted Effluent
1467 Spots

Average for all Top 6:
1399 Spots

Average for all Top 14:
1451 Spots

Figure 7. **2-D DIGE images of crude and depleted effluent samples**. Top 14 depleted samples showed the most protein spots and produced a similar protein spot map to the top 6 depleted sample that was previously used to identify putative protein biomarkers.

We ran a 'pick' gel to identify these 27 protein spots. We have had staff turnover the last three months, so we were not able to complete the protein identification. We have determined an appropriate schedule for the final quarter of this project to finish this part of the project. We assessed the differentially expressed proteins using principle component analysis (PCA) and hierarchical clustering analysis. The PCA analysis shows dramatic differences between the two types of affinity removal and hierarchical clustering showed that both techniques could produce clustering of wound healing as well as clustering of the technique used. PCA (panel A) and clustering (panel B) are shown in Figure 21.

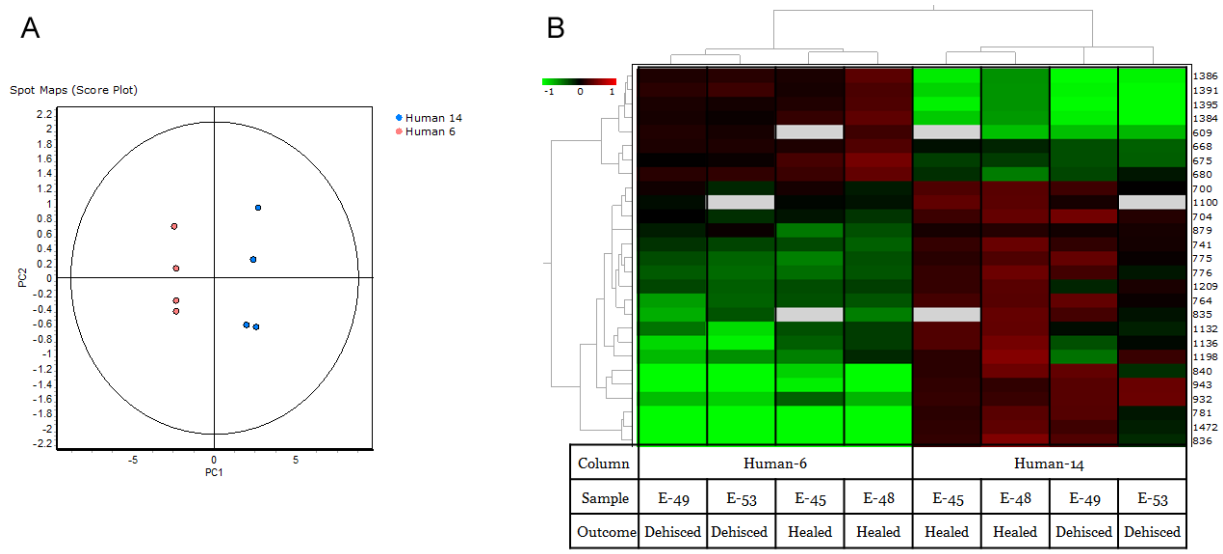

Figure 8. **PCA analysis and hierarchical clustering** show that top 14 protein removal from wound effluent will likely produce appropriate wound healing biomarkers. A. PCA analysis shows that the four top 6 samples are most similar to each other and the 4 top 14 samples are most similar to each other. B. Hierarchical clustering shows that there are groups of protein spots that are similarly expressed between column types and between healed vs. dehisced samples.

Task 5. Assays utilizing the microbead platform will be discovered and verified for microbead platform compatibility for novel host protein biomarkers in wound exudates, debridement tissue, and plasma of wound patients.

The proteomics analysis at UC Davis has implicated the following three proteins as potential biomarkers: serum amyloid P, ceruloplasmin, and complement C3. Although we did not complete this task, we made substantial progress towards the eventual use of microbead platform compatibility. Using the panel of wound effluent markers found in Task 4, we determined which of these markers had appropriate microbead antibodies. We purchased these antibodies and ran ELISA (Enzyme linked immunosorbant assays) to validate the differential protein expression in our full sample set. We completed ELISA experiments for 3 of the 9 proteins in the marker panel for wound effluent. Unfortunately, we were not able to assess data from these samples due to 2 main issues: A) We had a staffing issue in the last six months of the project where the technician working on these assays left UC Davis to pursue a job in industry. Since there was not enough time to hire a new employee in this last period, we began to train an undergraduate to complete the ELISAs and to have a faculty scientist complete this work. The training of the new person, as well as organizing the samples and data following the departure of the technician proved to be more difficult than anticipated. We were not able to finish all the data analysis for this task by the end of the performing period. Our hope is that we will be able to secure additional funding and finish this part of the work. The second issue; B) Of the 9 protein spots that show differential expression that lead to the highly successful discrimination between healed and non-healed wounds, 3 of these are complement C3. These proteins are distinct in the 2-D DIGE analysis, but when using antibodies for ELISA (or microbead) it is not clear from the existing data which of them or potentially all three of them are represented by the antibody-dependent ELISA data. Further analysis of the particular protein spots found on the gels, and the particular complement

C3 species detected by the antibody-based assay techniques. This analysis was started, but we were not able to finish this by the end of the project, due to the complexity of the analysis and the amount of mass spectrometry data that is needed to discriminate between the different complement C3 proteins found in the 2-D DIGE experiments. We hope to obtain additional funds regarding these complement C3 isoforms and better determine how they relate to a future biomarker panel containing these protein isoforms.

Task 6. In addition to addressing issues on the "clinical science" of wound healing in the tasks above, this project will aim to significantly improve on the analytical technological methods (such as multiplex PCR) and streamlined clinical instrumentation (such as the Luminex MagPix system or the lower cost field-hardened Parallel Synthesis Technologies MARS reader) for detecting both nucleic acid and protein analytes in the same wound samples.

Due to issues raised above for task 5 and for other issues (see aim 1 tasks), we were not able to make significant progress on this task. However, we were able to clearly indicate that data collected from both pathogen DNA and host protein could be correlated and could begin to be assessed from the same wound samples.

AIM 3: DATA ANALYSIS AND CLINICAL CORRELATIONS

Task 7. The bioinformatics analysis of the 454 metagenomics data will be validated.

With the technology advancement of next generation sequencing, Illumina sequencing has surpassed 454 sequencing in terms of throughput, quality of data and cost. Therefore, we used Illumina sequencing instead of 454 to analyze the samples in this study. The detailed sequencing analysis is described under Aim 1, Task 2. We were able to leverage a novel algorithm developed at LLNL, the Livermore Metagenomics Analysis Tool kit for bioinformatics analysis of the wound samples. The detailed SOP and algorithm development was described in a recent publication by Ames et al., 2013 (13).

Task 8. LLNL will construct statistical models to predict clinical outcomes by integrating data on (i) identified microbial flora and (ii) host response biomarkers. Standard multivariate regression methods will be used to predict categorical responses (wound closure *vs* acute infection *vs* chronic infection), and a Cox proportional hazard model will be applied to predict quantitative measures such as time to closure.

Association of microbial species detection with wound outcome. Microorganisms detected in each wound sample were examined with respect to the ultimate clinical outcome of the wound. Fifty-four samples (44% of total) were derived from wounds that failed to heal. LLMDA detection status for each individual sample is shown in Figure 9, along with clinical outcome of the corresponding wound (green = healed, red = failed). Samples were clustered according to microbial profile as detected by LLMDA (see publication Be et al. for complete analysis methods).

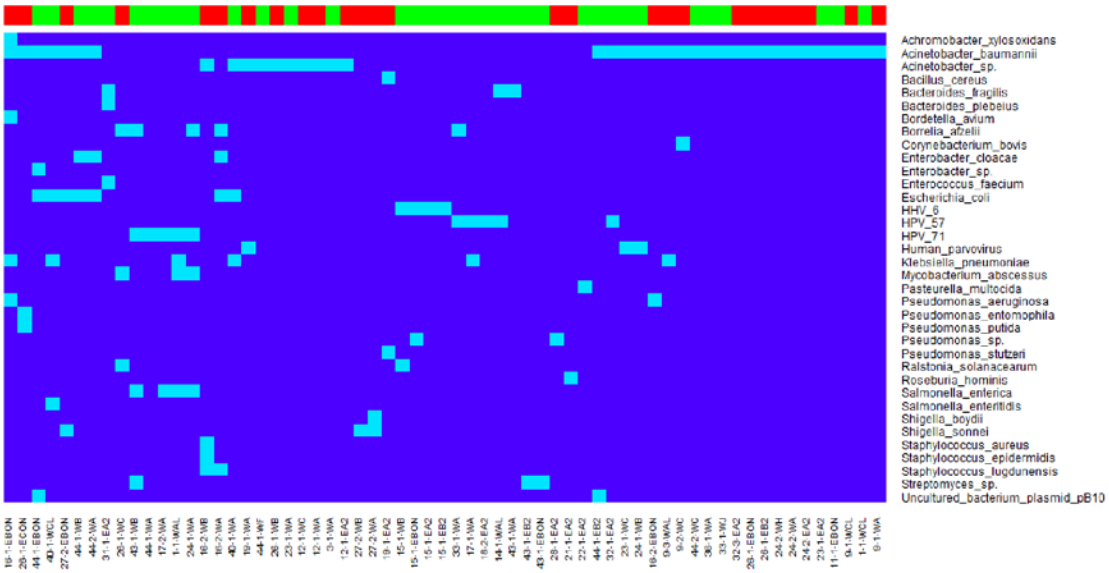

Figure 9. Clustering of samples from healed and dehisced combat wounds according to microbial species detected by microarray.

Samples derived from wounds with the same outcome did not cluster together in all cases, thus outcome could not be predicted based on complete microbial profile. Detection of specific microbial targets did, however, associate with outcome (Table 7). *A. baumannii* were detected by LLMDA in 14% of effluent samples from healed wounds, compared to 27% for dehisced wounds. This association with wound failure was not statistically significant (P=0.150), though a larger sample set could provide additional statistical power. LLMDA detected *Pseudomonas* in 3% of effluent samples from healed wounds, and 17% of samples from failed wounds (P=0.059). Overall, *Pseudomonas* were detected in 3% of healed wounds and 23% of failed wounds (P=0.020). Paradoxically, an inverse correlation was observed with detection of bacterial species associated with the gastrointestinal system. These organisms were detected most commonly in tissue samples, in which 30% of samples from healed wounds contained one or more of these species, as compared to only 4% in those from failed wounds (P=0.013).

Association of Acinetobacter *sequence-specific detection with wound resolution.* The microarray platform also confers the ability to detect bacterial plasmids. *Acinetobacter* plasmid pRAY was the most commonly detected plasmid. pRAY was detected in only 3% of healed effluent samples, compared to 23% of failed samples (P=0.012). In tissue samples, pRAY was detected in 24% of healed samples and 42% of failed wound samples (P=0.134). Overall, pRAY was detected in 15% of healed wounds and 41% of failed wounds (P=0.029).

	All samples			Individual wounds		
Category	**Healed (%)**	**Dehisced (%)**	**P**	**Healed (%)**	**Dehisced (%)**	**P**
All				39 (63.9%)	22 (36.1%)	
Effluent	37 (55.2%)	30 (44.8%)				
Tissue	33 (57.9%)	24 (42.1%)				
Culture				14 (35.9%)	11 (50.0%)	0.210
Effluent	7 (18.9%)	8 (26.7%)	0.321			
Tissue	16 (48.5%)	11 (45.8%)	0.528			
LLMDA				19 (48.7%)	13 (59.1%)	0.305
Effluent	13 (35.1%)	12 (40.0%)	0.437			
Tissue	23 (69.7%)	15 (62.5%)	0.386			
A. baumannii				10 (25.6%)	9 (40.9%)	0.171
Effluent	5 (13.5%)	8 (26.7%)	0.149			
Tissue	9 (27.3%)	6 (25.0%)	0.548			
Acinetobacter pRAY				6 (15.4%)	9 (40.9%)	0.029
Effluent	1 (2.7%)	7 (23.3%)	0.012			
Tissue	8 (24.2%)	10 (41.7%)	0.134			
Pseudomonas				1 (2.6%)	5 (22.7%)	0.020
Effluent	1 (2.7%)	5 (16.7%)	0.059			
Tissue	0 (0.0%)	0 (0.0%)				
Enteric bacteria				9 (23.1%)	2 (9.1%)	0.155
Effluent	2 (5.4%)	1 (3.3%)	0.579			
Tissue	10 (30.3%)	1 (4.2%)	0.013			

Table 7. Correlation of target detection by microarray with wound resolution status.

Functional analysis of protein expression data. We also (for the first time) parameterized raw protein expression data from all wound effluent samples to be used in the draft functional network model. This data transformation is of interest to the company that supplies the proteomics data analysis software and we are in the process of writing an application note to enable other proteomic data of this nature to be used in subsequent network models. We were also able to contribute this host protein data to the network model being developed at LLNL to continue data analysis integration of host protein and pathogen nucleic acids.

Addition work that was not part of the original SOW: initial functional modeling of wound biomarker measurements and wound outcome

By year 3 of the research study, we have collected a comprehensive set of microbial and wound biomarker data, as well as clinical data related to wound healing and patient information. The logical next step of the research study is to develop a computation al network model to integrate this comprehensive set of markers and perform functional modeling to predict wound outcome. This model would impact clinical decisions and lead to better wound care and treatment. We submitted a proposal to the MIDRP Clinical Trial Award but unfortunately the proposal was not selected for funding. Here is a description of our preliminary analysis using computational modeling to predict outcome:

We performed mutual information network analysis (MINA) of the wound outcome data combined with effluent protein biomarker measurements obtained by 2D-DIGE. Mutual information (MI) is a statistical measure that quantifies the extent to which knowing the value of one variable predicts the value of another. For continuous data it serves a similar role to a correlation coefficient; unlike correlation, however, it can be applied to mixtures of continuous and discrete variables. The main benefit of MI analysis is that it can show dependency

relationships between sets of variables, regardless of whether the variables are positively or negatively correlated.

We computed MI between all pairs of variables (protein spot volumes and wound healing outcome), converted the MI values to normalized distances between variables, and used the distances to cluster the variables using the topological data analysis (TDA) tool Ayasdi Iris (21). The resulting MI network is shown in Figure 10. Each node in the network represents a group of variables that are strongly correlated or anti-correlated, and nodes that are linked indicate moderate correlations. Nodes are colored according to the number of variables contained within them (more for red, less for green and blue), except for the segment of the network shown in white, which groups the protein spots that are most strongly associated with healing outcome. There are 108 spots in this segment, 18 of which were identified as belonging to specific proteins (see Table 8). The t-scores shown for each identified spot in the table indicate the direction of the relationship between spot volume and outcome; for example, spot 102 (ubiquitin carboxyl terminal hydrolase 32) was strongly correlated with dehiscence, and spot 852 (alpha-1-antichymotrypsin) correlated with successful healing. Identification of additional spots and profiling of protein levels across a larger set of wound samples will be needed to elucidate the interrelationships between protein levels and wound healing mechanisms.

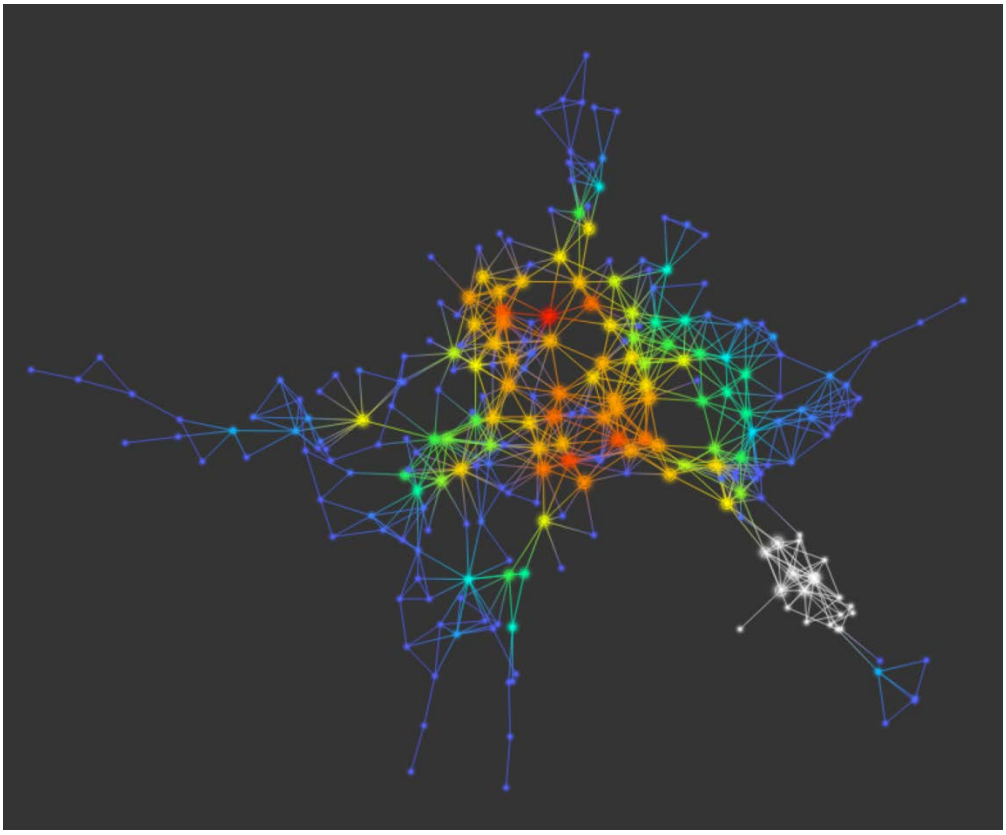

Figure 10: Mutual information network for wound healing outcome and DIGE protein spot measurements. Each node in the network represents a group of variables that are strongly correlated or anti-correlated.

Spot number	Protein	T-score (dehisced vs healed)
102	Ubiquitin carboxyl terminal hydrolase 32	2.45
814	Isoform 5 of Interleukin enhancer binding factor 3	1.85
106	Isoform 2 of Poly (ADP-ribose) glycohydrolase	1.4
387	Leukocyte immunoglobin-like receptor subfamily B	1.14
1778	Isoform 1 of Inter-alpha-trypsin inhibitor	1.14
1576	Alpha-1-acid glycoprotein 1	0.81
257	Isoform 1 of Inter-alpha-trypsin inhibitor	0.43
250	Isoform 1 of Inter-alpha-trypsin inhibitor	0.3
209	Ceruloplasmin	0.12
232	Platelet endothelial aggregational receptor 1	-0.27
117	Complement factor H	-0.3
1119	Isoform 2 of Na-dependent phosphate transporter protein 3	-0.44
358	Complement C3	-0.98
353	Complement C3	-1.11
1080	Zinc alpha 2 glycoprotein precursor	-1.16
1142	Complement component C9	-1.22
981	HLA class 1 histocompatibility antigen	-1.58
852	Isoform 1 of alpha-1-antichymotrypsin	-3.93

Table 8: Identified protein spots associated with healing outcome by MI analysis

KEY RESEARCH ACCOMPLISHMENTS

Aim 1:

- Optimized protocols for molecular analysis of wound samples via microarray and sequencing
- Performed microbial analysis of 124 unique combat wound samples via microarray
- Achieved species level microbial detection by microarray in 51% of wound samples, including in 31% of samples identified as culture-negative by standard microbiology, validating this technology as a rapid, comprehensive method for assessment of microbial infection
- Performed microbial analysis of 21 unique combat wound samples via next-generation sequence analysis
- Undertook sequence analysis to examine bioburden diversity and temporal shifts throughout the course of treatment
- Designed PCR detection signatures for the most relevant detected organisms, yielding a detection tool that could be rapidly applied in a diagnostic environment

Aim 2:

- Determined ideal sample quantity and storage medium prior to analysis via 2-D DIGE.
- Optimized sample preparation methods and run parameters for 2-D DIGE.

- Determined that a large quantity of protein spots are obtained following analysis of preliminary burn wound samples.
- Optimized high abundant protein removal from both serum and wound effluent for 2-D DIGE analysis.
- Discovered 9 protein biomarkers that discriminate between healing and non-healing wounds.
- Determined removal of 14 high abundant proteins may provide additional lower abundance biomarkers in wound effluent.

Aim 3

- Identified multiple previously unknown associations between detection of specific microbial sequence targets and wound healing failure
- Identified a significant association between enteric bacterial colonization and *improved* wound healing
- Developed a preliminary computational network modeling approach and performed early testing using this algorithm to correlate protein biomarkers with wound outcome

REPORTABLE OUTCOMES

Publications:

Be NA, Allen JE, Brown TS, Gardner SN, McLoughlin KS, Forsberg JA, Kirkup BC, Chromy BA, Luciw PA, Elster EA, Jaing CJ. Microbial profiling of combat wound infection through detection microarray and next-generation sequencing. Submitted (Status: revise and resubmit).

Chromy BA, Eldridge A, Forsberg JA, Brown TS, Kirkup BC, Elster E, Luciw P. Proteomic sample preparation for blast wound characterization. Proteome Science 12(1):10. doi:10.1186/1477-5956-12-10. http://www.proteomesci.com/content/12/1/10

Chromy BA, Eldridge A, Forsberg J, Brown TS, Kirkup BC, Jaing C, Be NA, Elster E, Luciw PA. 2013. Wound outcome in combat injuries is associated with a unique set of protein biomarkers. Journal of Translational Medicine 11(1):281. doi:10.1186/1479-5876-11-281. http://www.translational-medicine.com/content/11/1/281

Chromy BA, Eldridge A, Forsberg J, Brown TS, Kirkup BC, Jaing C, Be NA, Elster E, Luciw PA. 2013. Serum protein biomarkers in combat injuries predict wound outcome. (In preparation)

Application Note. GE Healthcare. 2-D DIGE DeCyder protein quantification data transformed into Microsoft Excel for additional data analysis. (In preparation)

Dastgheyb N, Eldridge A, Luciw PA, Sen S, Chromy BA, Proteomic Analysis of Healthy and Injured Human Skin (Status: revise and resubmit).

Proposals submitted:

"Integration of functionally predictive host immune biomarker and microbial assays with network modeling for guidance of wound therapy" (DM140389) in response to W81XWH-14-DMRDP-MID-CTA, FY14-17. Not funded.

"Comprehensive characterization of pathogens and host markers for effective wound treatment" (Log #. 13032001) in response to USAMRMC BAA13-1, not invited.

Invited oral presentations:

Jaing C., Military Infectious Disease Research Program (JPC2) In Progress Review, March 28, 2013, Ft. Detrick. MD.

Be NA, Chromy BA, Brown TS, Eldridge A, Gardner SN, McLoughlin KS, Luciw PA, Elster EA, Jaing C. Profiling of combat wounds through microbial and host biomarker detection. In: Gordon Research Seminar: Chemical and Biological Terrorism Defense; Ventura, CA; 2013 Mar 9-10.

Poster presentations at professional meetings:

Be NA, Brown TS, Chromy BA, Eldridge A, Gardner SN, McLoughlin KS, Luciw PA, Elster EA, Jaing C. Profiling of combat wounds through microbial and host biomarker detection. 113th Annual Meeting, American Society for Microbiology; Denver, CO; 2013 May 18-21; Abstract 1849.

Be NA, Brown TS, Chromy BA, Gardner SN, McLoughlin KS, Elster EA, Jaing C. Detection of microbial colonization in combat wounds. In: Military Health System Research Symposium; Fort Lauderdale, FL; 2012 Aug 13-16; Abstract 4, Infection Control and Treatment.

Be NA, Gardner S, McLoughlin K, Thissen JB, Slezak T, Jaing C. A comprehensive microbial detection array applied to biodefense and public safety. In: 5th National Bio-Threat Conference; Denver, Colorado; 2012 March 27-29.

CONCLUSION

The results of this study demonstrate the utility of employing advanced genomic and proteomic technologies for revealing powerful clinical metrics not attainable through the current standard of care. Through application of microarray, sequencing, and 2D-DIGE platforms, we have identified a broad range of wound-relevant pathogens and host biomarkers. Detection of microorganisms in wounds believed to be culture-negative in this study would be critically relevant to treatment of these injuries. Similarly, the comprehensive and unbiased nature of our proteomics analysis yielded a previously unidentified set of biomarkers that are indicative of the host response and predictive of wound healing progress. In combination, these microbial and host profiles provide essential and previously unknown data toward development of novel diagnostics for wound characterization and clinical outcome classification.

Taken together, these data support the inclusion of integrated molecular techniques alongside the standard of care for wound diagnostics. Clinical assessment of the microbial flora

and protein microenvironment unique to each wound in each patient would provide invaluable clinical information throughout the treatment process. More effective and timely assessments based on quantifiable metrics would reduce surgical morbidity, accelerate rehabilitation, and decrease length of hospital stays. The potential for reduction in overall healthcare costs further supports the application of these molecular platforms as a prudent and cost-effective addition to the wound diagnostics armamentarium. These techniques could represent an important step toward personalized assessment of individual patients and rational design of tailored treatment regimens.

REFERENCES

1. Hawksworth JS, Stojadinovic A, Gage FA, Tadaki DK, Perdue PW, Forsberg J, Davis TA, Dunne JR, Denobile JW, Brown TS, et al. Inflammatory biomarkers in combat wound healing. *Ann Surg.* 2009;250(6):1002-7.
2. Brown TS, Hawksworth JS, Sheppard FR, Tadaki DK, and Elster E. Inflammatory response is associated with critical colonization in combat wounds. *Surg Infect (Larchmt).* 2011;12(5):351-7.
3. Evans KN, Forsberg JA, Potter BK, Hawksworth JS, Brown TS, Andersen R, Dunne JR, Tadaki D, and Elster EA. Inflammatory cytokine and chemokine expression is associated with heterotopic ossification in high-energy penetrating war injuries. *J Orthop Trauma.* 2012;26(11):e204-13.
4. Bowler PG, Duerden BI, and Armstrong DG. Wound microbiology and associated approaches to wound management. *Clin Microbiol Rev.* 2001;14(2):244-69.
5. McGuckin M, Goldman R, Bolton L, and Salcido R. The clinical relevance of microbiology in acute and chronic wounds. *Adv Skin Wound Care.* 2003;16(1):12-23; quiz 4-5.
6. Davis SC, Ricotti C, Cazzaniga A, Welsh E, Eaglstein WH, and Mertz PM. Microscopic and physiologic evidence for biofilm-associated wound colonization in vivo. *Wound Repair Regen.* 2008;16(1):23-9.
7. Hurlow J, and Bowler PG. Clinical experience with wound biofilm and management: a case series. *Ostomy Wound Manage.* 2009;55(4):38-49.
8. Ryan TJ. Infection following soft tissue injury: its role in wound healing. *Curr Opin Infect Dis.* 2007;20(2):124-8.
9. Frankel YM, Melendez JH, Wang NY, Price LB, Zenilman JM, and Lazarus GS. Defining wound microbial flora: molecular microbiology opening new horizons. *Arch Dermatol.* 2009;145(10):1193-5.
10. Forsberg JA, Elster EA, Andersen RC, Nylen E, Brown TS, Rose MW, Stojadinovic A, Becker KL, and McGuigan FX. Correlation of procalcitonin and cytokine expression with dehiscence of wartime extremity wounds. *J Bone Joint Surg Am.* 2008;90(3):580-8.
11. Gardner S, Jaing C, McLoughlin K, and Slezak T. A microbial detection array (MDA) for viral and bacterial detection. *BMC Genomics.* 2010;11(1):668.
12. Dowd SE, Sun Y, Secor PR, Rhoads DD, Wolcott BM, James GA, and Wolcott RD. Survey of bacterial diversity in chronic wounds using pyrosequencing, DGGE, and full ribosome shotgun sequencing. *BMC Microbiol.* 2008;8(43.

13. Ames SK, Hysom DA, Gardner SN, Lloyd GS, Gokhale MB, and Allen JE. Scalable metagenomic taxonomy classification using a reference genome database. *Bioinformatics.* 2013.
14. Krylov V, Shaburova O, Krylov S, and Pleteneva E. A genetic approach to the development of new therapeutic phages to fight pseudomonas aeruginosa in wound infections. *Viruses.* 2012;5(1):15-53.
15. Mihu MR, and Martinez LR. Novel therapies for treatment of multi-drug resistant Acinetobacter baumannii skin infections. *Virulence.* 2011;2(2):97-102.
16. Gardner SN, and Slezak T. Scalable SNP Analyses of 100+ Bacterial or Viral Genomes. *Journal of Forensic Research.* 2010;1(107.
17. Gardner SN. When Whole-Genome Alignments Just Won't Work: kSNP v2 Software for Alignment-Free SNP Discovery and Phylogenetics of Hundreds of Microbial Genomes. *PLoS ONE.* 2013;8(12):e81760.
18. Hysom D, Naraghi-Arani P, Elsheikh M, Carrillo AC, Williams P, and Gardner SN. Skip the Alignment: Degenerate, Multiplex Primer and Probe Design Using K-mer Matching Instead of Alignments. *PLoS ONE* 2012;7(4):e34560.
19. Chromy B, Eldridge A, Forsberg J, Brown T, Kirkup B, Elster E, and Luciw P. Proteomic sample preparation for blast wound characterization. *Proteome Science.* 2014;12(1):10.
20. Chromy B, Eldridge A, Forsberg J, Brown T, Kirkup B, Jaing C, Be N, Elster E, and Luciw P. Wound outcome in combat injuries is associated with a unique set of protein biomarkers. *Journal of Translational Medicine.* 2013;11(1):281.
21. Lum PY, Singh G, Lehman A, Ishkanov T, Vejdemo-Johansson M, Alagappan M, Carlsson J, and Carlsson G. Extracting insights from the shape of complex data using topology. *Scientific reports.* 2013;3(1236.

SUPPORTING DATA

Table S1. Microorganisms detected by LLMDA in all wound tissue and effluent samples.

NG = no growth, UNK = unknown culture status
*Organism detected by LLMDA at lower intensity threshold (0.95)

Wound sample ID	Type	Outcome	Culture results	LLMDA detection
1-1-WAL	Tissue	Healed	Pseudomonas stutzeri	Mycobacterium abscessus* Salmonella enterica* Klebiella pneumoniae* HPV 71*
1-1-WCL	Tissue	Healed	Citrobacter freundii	Acinetobacter sp. SUN plasmid pRAY
2-1-EA2	Effluent	Healed	UNK	None detected
2-2-EA2	Effluent	Healed	NG	None detected
3-1-EA2	Effluent	Healed	NG	None detected
3-1-WA	Tissue	Healed	NG	Acinetobacter sp. SUN plasmid pRAY
4-1-EA2	Effluent	Healed	NG	None detected
5-1-EA2	Effluent	Healed	NG	None detected
6-1-EA2	Effluent	Dehisced	NG	None detected
6-2-EA2	Effluent	Healed	NG	None detected
7-1-EA2	Effluent	Healed	NG	None detected
8-1-EA2	Effluent	Healed	NG	None detected
9-1-WA	Tissue	Dehisced	Acinetobacter baumannii	Acinetobacter sp. SUN plasmid pRAY Acinetobacter baumannii plasmid pACICU2* Acinetobacter baumannii plasmid pABIR
9-1-WCL	Tissue	Dehisced	Acinetobacter baumannii	Acinetobacter sp. 6014059 Acinetobacter sp. SUN plasmid pRAY Acinetobacter baumannii ACICU plasmid pACICU2 Acinetobacter baumannii plasmid pABIR
9-2-WC	Tissue	Dehisced	Acinetobacter baumannii	Acinetobacter baumannii plasmid pABIR Acinetobacter sp. SUN plasmid pRAY Acinetobacter baumannii ACICU plasmid pACICU2 Corynebacterium bovis
9-3-WAL	Tissue	Dehisced	Acinetobacter baumannii	Acinetobacter sp. SUN plasmid pRAY Acinetobacter baumannii plasmid pACICU2* Acinetobacter baumannii plasmid pABIR Klebsiella pneumoniae plasmid*
10-1-WAL	Tissue	Healed	NG	None detected
10-1-WF	Tissue	Healed	Acinetobacter baumannii Enterococcus faecium	None detected
11-1-EB2	Effluent	Healed	NG	None detected

11-1-EBON	Effluent	Healed	NG	Acinetobacter sp. 6014059 Acinetobacter baumannii plasmid pACICU Acinetobacter baumannii plasmid pAB0057 Acinetobacter baumannii AB0057 Acinetobacter baumannii plasmid pMMA2 Acinetobacter baumannii ATCC 17978 plasmid pAB2 Salmonella enterica
11-1-WB	Tissue	Healed	NG	None detected
12-1-EA2	Effluent	Dehisced	Acinetobacter baumannii	Acinetobacter sp. SUN plasmid pRAY
12-1-WA	Tissue	Dehisced	Acinetobacter baumannii	Acinetobacter sp. SUN plasmid pRAY
12-1-WC	Tissue	Dehisced	UNK	Acinetobacter sp. SUN plasmid pRAY
13-2-EB2	Effluent	Dehisced	NG	None detected
13-2-EBON	Effluent	Dehisced	NG	None detected
13-2-WB	Tissue	Dehisced	NG	None detected
14-1-WAL	Tissue	Healed	Escherichia coli	Bacteroides fragilis NCTC 9343*HPV 57*
14-1-WC	Tissue	Healed	NG	None detected
15-1-EA2	Effluent	Healed	NG	HHV 6
15-1-EB2	Effluent	Healed	NG	HHV 6
15-1-EBON	Effluent	Healed	NG	HHV 6 Pseudomonas sp. S-47 plasmid p47S*
15-1-WA	Tissue	Healed	NG	None detected
15-1-WB	Tissue	Healed	NG	Ralstonia solanacearum* HHV 6
16-1-EA2	Effluent	Dehisced	NG	None detected
16-1-EB2	Effluent	Dehisced	Stenotrophomonas maltophilia	None detected
16-1-EBON	Effluent	Dehisced	Stenotrophomonas maltophilia	Pseudomonas aeruginosa PAb1 Pseudomonas aeruginosa C3719 Pseudomonas aeruginosa PAO1 Pseudomonas aeruginosa UCBPP-PA14 Pseudomonas aeruginosa PACS2 Bordetella avium 197N Achromobacter xylosoxidans A8 Acinetobacter baumannii AB0057 plasmid pAB0057* Klebsiella pneumoniae MGH78578*
16-1-WA	Tissue	Dehisced	NG	None detected
16-1-WB	Tissue	Dehisced	Stenotrophomonas maltophilia	None detected
16-2-EA2	Effluent	Dehisced	NG	None detected
16-2-EB2	Effluent	Dehisced	NG	None detected
16-2-EBON	Effluent	Dehisced	NG	Acinetobacter sp. 6013113 Acinetobacter baumannii sp. SUN plasmid pRAY Acinetobacter baumannii SDF Acinetobacter baumannii plasmid pMMA2 Pseudomonas aeruginosa PAb1 Pseudomonas aeruginosa C3719 Pseudomonas aeruginosa PAO1
16-2-WA	Tissue	Dehisced	NG	Enterobacter cloacae plasmid pEC01 Escherichia coli plasmid pIGRW12 Staphylococcus lugdunensis 995 plasmid pLUG10* Borrelia afzelii Pko*

16-2-WB	Tissue	Dehisced	NG	Acinetobacter sp. SUN plasmid pRAY Staphylococcus epidermidis Staphylococcus lugdunensis Staphylococcus aureus*
17-1-WA	Tissue	Healed	Enterococcus faecium	Klebsiella pneumoniae plasmid* HPV 57*
17-1-WB	Tissue	Healed	NG	None detected
17-2-EA2	Effluent	Healed	Enterococcus faecium	None detected
17-2-WA	Tissue	Healed	Enterococcus faecium	Salmonella enterica* HPV71*
17-2-WB	Tissue	Healed	NG	None detected
18-1-EA2	Effluent	Dehisced	NG	None detected
18-1-WA	Tissue	Dehisced	NG	None detected
18-1-WB	Tissue	Dehisced	Enterococcus faecium	None detected
18-2-EA2	Effluent	Healed	NG	HPV57*
19-1-EA2	Effluent	Dehisced	Bacillus cereus Acinetobacter sp.	Bacillus cereus AH676 Pseudomonas stutzeri DSM4166*
19-1-WA	Tissue	Dehisced	Acinetobacter sp. Bacillus cereus	Acinetobacter sp. SUN plasmid pRAY Human parvovirus B19
19-2-EA2	Effluent	Dehisced	Acinetobacter sp.Alloicoccus otidis	None detected
19-2-WA	Tissue	Dehisced	Acinetobacter sp. Alloicoccus otidis	None detected
20-1-EA2	Effluent	Dehisced	NG	None detected
20-2-EA2	Effluent	Dehisced	NG	None detected
21-1-EA2	Effluent	Dehisced	NG	Roseburia hominis A2−183*
21-2-EA2	Effluent	Dehisced	NG	None detected
22-1-EA2	Effluent	Healed	NG	Pasteurella multocida 381 plasmid pCCK381*
23-1-EA2	Effluent	Healed	Acinetobacter baumannii/calcoaceticus complex	Acinetobacter sp. 6013113 Acinetobacter baumannii TCDC Acinetobacter baumannii sp. SUN plasmid pRAY Acinetobacter baumannii ATCC 27244 Acinetobacter baumannii ATCC 17978 plasmid pAB1 Acinetobacter baumannii ACICU
23-1-WA	Tissue	Healed	Acinetobacter baumannii/calcoaceticus complex	Acinetobacter sp. SUN plasmid pRAY
23-1-WC	Tissue	Healed	NG	Acinetobacter sp. SUN plasmid pRAY Acinetobacter baumannii ATCC 17978 plasmid pAB1 Human parvovirus B19
24-1-WA	Tissue	Healed	Acinetobacter baumannii	Mycobacterium abscessus* HPV 71 * Salmonella enterica* Borrelia afzelii*
24-1-WB	Tissue	Healed	NG	Acinetobacter sp. SUN plasmid pRAY Acinetobacter baumannii plasmid pABIR Human parvovirus B19
24-2-EA2	Effluent	Dehisced	Acinetobacter baumannii	Acinetobacter sp. 6013150 Acinetobacter sp. SUN plasmid pRAY Acinetobacter baumannii AB307-0294
24-2-WA	Tissue	Dehisced	Acinetobacter baumannii	Acinetobacter sp. SUN plasmid pRAY Acinetobacter baumannii ACICU plasmid pACICU

24-2-WH	Tissue	Dehisced	NG	Acinetobacter baumannii AB0057 plasmid pAG0057 Acinetobacter baumannii AYE plasmid p4ABAYE Acinetobacter baumannii ATCC 17978 plasmid pAB2
25-1-EA2	Effluent	Healed	NG	None detected
26-1-EA2	Effluent	Dehisced	NG	None detected
26-1-EB2	Effluent	Dehisced	Staphylococcus capitis	Acinetobacter sp. SUN plasmid pRAY* Acinetobacter baumannii plasmid pMMA2*
26-1-EBON	Effluent	Dehisced	Staphylococcus capitis	Acinetobacter sp. 6013113 Acinetobacter sp. SUN plasmid pRAY Acinetobacter baumannii SDF Acinetobacter baumannii plasmid pMMA2
26-1-ECON	Effluent	Dehisced	NG	Acinetobacter sp. 6013113 Acinetobacter sp. SUN plasmid pRAY Acinetobacter baumannii SDF Acinetobacter baumannii plasmid pMMA2 Pseudomonas putida F1 Pseudomonas entomophila L48 Pseudomonas putida GB-1
26-1-WA	Tissue	Dehisced	NG	None detected
26-1-WB	Tissue	Dehisced	Staphyllococcus capitis	Acinetobacter sp. SUN pRAY
26-1-WC	Tissue	Dehisced	NG	Ralstonia solanacearum* Mycobacterium abscessus* Borrelia afzelii PKo*
27-1-EA2	Effluent	Healed	NG	None detected
27-2-EA2	Effluent	Dehisced	NG	None detected
27-2-EBON	Effluent	Dehisced	NG	Acinetobacter sp. 6013150Acinetobacter baumannii plasmid ACICUAcinetobacter baumannii plasmid pAB0057Acinetobacter baumannii sp. SUN plasmid pRAYAcinetobacter baumannii AB307-0294Acinetobacter baumannii plasmid pAB2Escherchia coli MS200-1*Escherchia coli E24377A plasmid pETEC74*Shigella sonnei 53G plasmid D*
27-2-WA	Tissue	Dehisced	NG	Shigella sonnei 53G plasmid D Shigella boydii CDC 30383-94 plasmid pBS512_2
27-2-WB	Tissue	Dehisced	NG	Shigella sonnei 53G plasmid D
28-1-EA2	Effluent	Dehisced	NG	Pseudomonas sp. S-47 plasmid p47S*
28-1-EB2	Effluent	Dehisced	NG	None detected
28-1-EBON	Effluent	Dehisced	NG	None detected
28-1-WA	Tissue	Dehisced	NG	None detected
28-1-WB	Tissue	Dehisced	NG	None detected
29-1-EA2	Effluent	Healed	NG	None detected
30-1-EA2	Effluent	Healed	UNK	None detected
31-1-EA2	Effluent	Healed	UNK	Bacteroides plebeius DSM 17135 Bacteroides fragilis NCTC 9343 Bacteroides fragilis plasmid pBFP35 Bacteroides fragilis WI1 plasmid pbHag−01 Enterococcus faecium TX0133C*
31-2-EA2	Effluent	Healed	UNK	None detected

32-1-EA2	Effluent	Healed	Acinetobacter baumannii	Acinetobacter sp. 6014059 Acinetobacter baumannii ACICU plasmid pACICU2 Acinetobacter baumannii AB307−0294 Human papillomavirus type 57
32-3-EA2	Effluent	Dehisced	NG	Acinetobacter baumannii plasmid pABIR
33-1-WA	Tissue	Healed	Acinetobacter baumannii Achromobacter sp.	HPV 57* Borrelia afzelii*
33-1-WJ	Tissue	Healed	NG	Acinetobacter baumannii plasmid pABIR
34-1-EB2	Effluent	Healed	NG	None detected
34-1-EBON	Effluent	Healed	NG	None detected
34-1-WA	Tissue	Healed	NG	None detected
34-1-WB	Tissue	Healed	NG	None detected
35-1-EA2	Effluent	Healed	NG	None detected
36-1-WA	Tissue	Healed	Acinetobacter baumannii	Acinetobacter baumannii AB0057 plasmid pAB0057 Acinetobacter baumannii plasmid pABVA01 Acinetobacter baumannii ATCC 17978 plasmid pAB2 Acinetobacter baumannii AYE plasmid p2ABAYE
37-1-EA2	Effluent	Healed	NG	None detected
37-2-EA2	Effluent	Healed	NG	None detected
38-1-EA2	Effluent	Healed	NG	None detected
38-1-WA	Tissue	Healed	NG	None detected
39-2-EA2	Effluent	Dehisced	UNK	None detected
40-1-WA	Tissue	Healed	Acinetobacter baumannii	Acinetobacter sp. SUN plasmid pRAY Escherichia coli plasmid p9123 Klebsiella pneumoniae plasmid pKpn114 Escherichia coli E24377A plasmid pETEC6
40-1-WCL	Tissue	Healed	Acinetobacter baumannii	Escherichia coli plasmid p9123Klebsiella pneumoniae plasmid pKpn114Salmonella enteritidis plasmid pKEscherichia coli E24377A plasmid pETEC_6Escherichia coli plasmid pVI678Acinetobacter sp. SUN plasmid pRAYAcinetobacter baumannii plasmid pABIR
41-1-EA2	Effluent	Healed	UNK	None detected
42-1-EA2	Effluent	Dehisced	NG	None detected
42-2-EA2	Effluent	Healed	NG	None detected
43-1-EA2	Effluent	Healed	NG	None detected
43-1-EB2	Effluent	Healed	Enterococcus faecium	*Streptomyces sp. x3 plasmid pTSC2
43-1-EBON	Effluent	Healed	Enterococcus faecium	*Streptomyces avermitilis *Streptomyces sp. x3 plasmid pTSC2
43-1-WA	Tissue	Healed	NG	Bacteroides fragilis IB143 plasmid pBI143
43-1-WB	Tissue	Healed	Enterococcus faecium	HPV 71* Salmonella enterica* Borrelia afzelii PKo* Streptomyces sp. AA4*
44-1-EB2	Effluent	Healed	Enterobacter cloacae Acinetobacter baumannii	Acinetobacter sp. 6014059 Acinetobacter baumannii ACICU plasmid pACICU2 Acinetobacter baumannii AB307-0294 Uncultured bacterium plasmid pB10

44-1-EBON	Effluent	Healed	Enterobacter cloacae Acinetobacter baumannii	Acinetobacter sp. 6014059 Acinetobacter baumannii ACICU plasmid pACICU2 Acinetobacter baumannii AB307-0294 Escherichia coli APEC O1 plasmid pAPEC-O1-R Enterobacter sp. W001 plasmi pR23 Uncultured bacterium plasmid pB10
44-1-WA	Tissue	Healed	Acinetobacter baumannii	HPV71*
44-1-WB	Tissue	Healed	Enterobacter cloacae Acinetobacter baumannii	Acinetobacter baumannii plasmid pABIR Enterobacter cloacae plasmid pEC01 Escherichia coli plasmid pIGRW12
44-1-WF	Tissue	Healed	NG	Acinetobacter sp. SUN plasmid pRAY
44-2-WA	Tissue	Healed	Acinetobacter baumannii	Acinetobacter sp. 6014059 Acinetobacter baumannii ACICU plasmid pACICU2 Acinetobacter baumannii AB307-0294 Enterobacter cloacae plasmid pEC01 Escherichia coli plasmid pIGRW12
44-2-WC	Tissue	Healed	NG	Acinetobacter baumannii plasmid pABIR